© 2020. Published by The Company of Biologists Ltd | Journal of Cell Science (2020) 133, jcs234914. doi:10.1242/jcs.234914

RESEARCH ARTICLE

CSB cooperates with SMARCAL1 to maintain telomere stability in ALT cells

Emily Feng, Nicole L. Batenburg, John R. Walker, Angus Ho, Taylor R. H. Mitchell, Jian Qin and Xu-Dong Zhu*

ABSTRACT

Elevated replication stress is evident at telomeres of about 10-15% of cancer cells, which maintain their telomeres via a homologous recombination (HR)-based mechanism, referred to as alternative lengthening of telomeres (ALT). How ALT cells resolve replication stress to support their growth remains incompletely characterized. Here, we report that CSB (also known as ERCC6) promotes recruitment of HR repair proteins (MRN, BRCA1, BLM and RPA32) and POLD3 to ALT telomeres, a process that requires the ATPase activity of CSB and is controlled by ATM- and CDK2-dependent phosphorylation. Loss of CSB stimulates telomeric recruitment of MUS81 and SLX4, components of the structure-specific MUS81-EME1-SLX1-SLX4 (MUS-SLX) endonuclease complex, suggesting that CSB restricts MUS-SLX-mediated processing of stalled forks at ALT telomeres. Loss of CSB coupled with depletion of SMARCAL1, a chromatin remodeler implicated in catalyzing regression of stalled forks, synergistically promotes not only telomeric recruitment of MUS81 but also the formation of fragile telomeres, the latter of which is reported to arise from fork stalling. These results altogether suggest that CSB-mediated HR repair and SMARCAL1-mediated fork regression cooperate to prevent stalled forks from being processed into fragile telomeres in ALT cells.

KEY WORDS: Cockayne syndrome group B protein, CSB, ERCC6, SMARCAL1, Replication stress, Homologous recombinational repair, Telomere fragility, Alternative lengthening of telomeres, ALT

INTRODUCTION

The nature of repetitive G-rich sequences represents an endogenous barrier for DNA replication fork progression at telomeres. If not resolved, this replication stress can drive telomere fragility, which manifests as multiple telomere signals per chromatid end seen in metaphase cells (Martinez et al., 2009; McKerlie et al., 2012; Sfeir et al., 2009). About 10-15% of human cancers rely on a homologous recombination (HR)-based mechanism, referred to as alternative lengthening of telomeres (ALT), to maintain their telomeres (Cesare and Reddel, 2010). In ALT cells, telomere transcription is deregulated and this deregulation can lead to enhanced collisions between replication and transcription complexes (Azzalin et al., 2007; Porro et al., 2010; Wilson et al., 2016), further contributing to replication stress at telomeres. Therefore, ALT telomeres represent a good experimental system to investigate genetic interactions that cancer cells rely on to resolve replication stress at their telomeres in order to support their continued growth and proliferation.

Department of Biology, McMaster University, Hamilton, Ontario, Canada L8S 4K1.

*Author for correspondence (zhuxu@mcmaster.ca)

X.-D.Z., 0000-0003-1859-3134

Received 30 May 2019; Accepted 13 January 2020

ALT cancer cells are characterized by several distinct hallmarks, including telomere length heterogeneity, a high level of extra-chromosomal telomeric DNA in the form of double-stranded linear/circular DNA or single-stranded circular DNA such as C-circles, elevated rates of telomeric sister chromatid exchange (T-SCEs) as well as PML bodies containing telomeric chromatin, referred to as ALT-associated PML bodies (APBs) (Henson and Reddel, 2010). These hallmarks are not always present together in ALT cells, indicative of the complexity of mechanisms that give rise to these features. Replication stress at telomeres is reported to trigger the processes leading to these hallmarks (Cox et al., 2016; Poole et al., 2015; Zhang et al., 2019b). DNA double-strand breaks (DSBs) induced at telomeres also drive ALT hallmarks (Dilley et al., 2016). Recently it has been reported that break-induced replication (BIR), a noncanonical form of homology-directed repair, drives telomere synthesis and promotes ALT hallmarks (Dilley et al., 2016; Zhang et al., 2019a,b). Not surprisingly, APBs are enriched with many proteins involved in DNA replication, recombination and repair such as DNA polymerase POLD3 (Dilley et al., 2016), an essential component of BIR, BLM (Stavropoulos et al., 2002), the MRE11/RAD51/NBS1 (MRN) complex (Wu et al., 2003, 2000), BRCA1, RAD51, RAD52 and RPA (Yeager et al., 1999).

SMARCAL1 is a chromatin remodeler that catalyzes branch migration and regression of stalled replication forks to protect stalled forks from collapsing (Bansbach et al., 2009; Betous et al., 2012; Yuan et al., 2009). SMARCAL1 is reported to resolve replication stress at telomeres in ALT cells (Cox et al., 2016; Poole et al., 2015). It has been reported that depletion of SMARCAL1 leads to persistently stalled replication forks at ALT telomeres (Cox et al., 2016), which are subject to cleavage by the structure-specific endonuclease MUS81-EME1-SLX1-SLX4 (MUS-SLX) complex (Fekairi et al., 2009; Hanada et al., 2007; Wyatt et al., 2013). It has also been reported that DSBs arising from collapsed forks as a result of cleavage by MUS-SLX are channelled into homology-directed BIR repair (Costantino et al., 2014; Roumelioti et al., 2016).

Cockayne syndrome group B (CSB) protein is encoded by the *ERCC6* gene, mutations of which account for the majority of cases of hereditary and devastating Cockayne syndrome (CS). CS is characterized by severe photosensitivity, physical impairment, neurological degeneration, muscle degeneration and premature aging (Laugel et al., 2009). Although CSB was first described to be involved in transcription-coupled nucleotide excision repair (Troelstra et al., 1992), many studies over the last few decades have revealed that CSB is a multifunctional protein that participates in a wide range of cellular processes. CSB is recruited to DSBs to regulate DSB repair pathway choice (Batenburg et al., 2015, 2017). At DSBs, CSB evicts histones and limits RIF1 accumulation in S/G2. In addition, CSB interacts with BRCA1 in late S/G2 to promote MRE11- and CtIP-mediated DNA end resection (Batenburg et al., 2019), thereby enforcing HR as the pathway choice of DNA DSB repair. It has been reported that CSB is associated with telomeres

Journal of Cell Science (2020) 133, jcs234914. doi:10.1242/jcs.234914

and that primary skin fibroblasts derived from CSB-deficient patients exhibit an increase in telomere fragility (Batenburg et al., 2012), indicative of a role of CSB in the resolution of replication stress at telomeres. However, how CSB resolves replication stress at telomeres remains poorly characterized.

In this report, we show that CSB localizes to ALT telomeres and this localization is stimulated by depletion of SMARCAL1, suggesting that stalled replication forks trigger CSB recruitment to ALT telomeres. We show that CSB promotes recruitment of the MRE11/RAD50/NBS1 complex, BRCA1, BLM, RPA32 and POLD3 to ALT telomeres in a manner that requires CSB's ATPase activity and is controlled by ATM- and CDK2-dependent phosphorylation. In addition, we demonstrate that CSB suppresses telomeric accumulation of MUS81 and SLX4, known to collapse stalled replication forks, suggesting that CSB limits MUS-SLX-mediated processing of stalled forks at ALT telomeres. Furthermore, loss of CSB coupled with depletion of SMARCAL1 leads to a synergistic increase in not only telomeric accumulation of MUS81 but also the formation of fragile telomeres. Taken together, these results suggest that CSB-mediated HR repair and SMARCAL1-mediated fork regression cooperatively prevent stalled forks from being processed into fragile telomeres. Loss of CSB combined with depletion of SMARCAL1 also results in a synergistical increase in chromatid breaks and micronuclei formation, which is associated with a synthetic reduction in cell proliferation, underscoring their concerted efforts to promote cell growth.

RESULTS

A commonly used CSB-deficient GM16095 cell line derived from a CS patient is an ALT cell line

GM16095, also known as SV40-transformed CS1AN (Troelstra et al., 1992), was derived from a CSB-deficient CS patient and is commonly used in laboratories working with CSB. We observed that while telomerase activity was readily detected in hTERT-immortalized GM10905 (hTERT-GM10905) cells, skin fibroblasts derived from a CSB-deficient CS patient (Batenburg et al., 2012), GM16095 cells did not exhibit any detectable telomerase activity (Fig. 1A), indicative of GM16095 being an ALT cell line. To gain further evidence that GM16095 might be an ALT cell line, we examined a number of ALT-associated hallmarks in GM16095 cells, including telomere length heterogeneity, t- and C-circles as well as ALT-associated PML bodies (APBs). Fluorescence *in situ* hybridization (FISH) analysis revealed that the telomere signal intensity on metaphase chromosome ends of GM16095 cells varied from barely detectable to fairly robust (Fig. 1B), indicative of telomere length heterogeneity. Southern blot analysis of telomere restriction fragments also revealed telomere length heterogeneity in GM16095 cells (Fig. S1B). In addition, GM16095 exhibited high levels of t-circles and C-circles (Fig. 1C,D). Furthermore, immunofluorescence (IF) analysis revealed the presence of APBs as evidenced by colocalization of telomeric DNA and TRF2 with PML bodies (Fig. 1E) in about 14-15% of asynchronous GM16095 cells. Taken together, these results demonstrate that GM16095 is an ALT cell line.

CSB regulates APB formation and C-circle production

Reintroduction of Myc-tagged wild-type CSB into GM16095 cells suppressed APB formation as evidenced by a reduction in colocalization of telomere binding protein TRF2 with PML bodies (Fig. 1F,G), although it did not affect the expression of TRF2 and PML (Fig. S1A). Reintroduction of Myc-CSB into GM16095 cells also suppressed C-circle production (Fig. 1H,I); however, it had little impact on telomere length heterogeneity (Fig. S1B). These results suggest that CSB regulates APB formation and C-circle production, hallmarks of ALT cells.

To further investigate if the effect of CSB on ALT features might be unique to the patient-derived GM16095 cell line, we also examined ALT features in human osteosarcoma U2OS, another well-established ALT cell line that is either wild type (WT) or knocked out (KO) for CSB. IF and IF-FISH analysis revealed that while telomeric DNA, TRF2 and phosphorylated (pT371)TRF1, the last of which has been reported to be a component of APBs (Wilson et al., 2016), were readily observed to colocalize with PML bodies in U2OS WT cells (Fig. 2A), loss of CSB led to an increase in the percentage of cells exhibiting their colocalization with PML bodies (Fig. 2B-D). This increase was unlikely due to any change in the expression of TRF2 or (pT371)TRF1 in U2OS CSB-KO cells (Fig. S1C). Loss of CSB also induced C-circle production (Fig. 2E,F); however, it had little impact on the rate of T-SCEs (E.F. and X.-D.Z., unpublished data). U2OS CSB-KO cells also did not exhibit any significant change in telomere length heterogeneity compared to U2OS WT cells despite continuous culturing (at least 1 month) (Fig. S1D). Reintroduction of Myc-CSB wild type into U2OS CSB-KO cells suppressed not only colocalization of PML bodies with telomeric DNA (Fig. 2G), TRF2 (Fig. S2A) and phosphorylated (pT371)TRF1 (Fig. S2B) but also C-circle production (Fig. S2C). Taken together, these results suggest that CSB regulates APBs and C-circles, two features thought to be best correlated with ALT cancers (Cesare and Reddel, 2010).

CSB requires its ATPase activity to regulate APB formation

CSB contains a central ATPase domain and therefore we asked if CSB might regulate APB formation through its ATPase activity. To address this question, we generated U2OS CSB-KO cells stably expressing the vector alone, Myc-tagged wild-type CSB or Myc-tagged CSB carrying a ATPase dead mutation of W851R (Batenburg et al., 2015). IF-FISH analysis revealed that while overexpression of Myc-CSB suppressed APB formation in U2OS CSB-KO cells, overexpression of Myc-CSB-W851R failed to do so (Fig. 2G). The expression of Myc-CSB-W851R was comparable to that of Myc-CSB (Fig. S2D). These results suggest that the ATPase activity of CSB is necessary to suppress APB formation.

Previously we have reported that CSB is phosphorylated on S10 by ATM and S158 by CDK2 and that these two phosphorylation events control its ATPase activity at DSBs *in vivo* (Batenburg et al., 2017). Therefore, we also investigated if CSB phosphorylation on S10 and S158 might regulate APB formation. We generated U2OS CSB-KO cells stably expressing the vector alone, Myc-CSB, Myc-CSB carrying a nonphosphorylatable S10A mutation, Myc-CSB carrying a phosphomimic S10D mutation, Myc-CSB carrying a nonphosphorylatable S158A mutation or Myc-CSB carrying a phosphomimic S158D mutation. IF-FISH analysis revealed that both Myc-CSB-S10D and Myc-CSB-S158D behaved like Myc-CSB wild type and suppressed APB formation whereas neither Myc-CSB-S10A nor Myc-CSB-S158A was able to do so (Fig. 2H). The inability of both Myc-CSB-S10A and Myc-CSB-S158A to suppress APB formation was unlikely due to any defect in their expression (Fig. S2E). These results suggest that CSB phosphorylation on S10 by ATM and S158 by CDK2 controls its ability to suppress APB formation.

CSB localizes to ALT telomeres and promotes telomeric recruitment of HR repair proteins

Telomeres in ALT cells are enriched with HR repair proteins. We have previously reported that CSB promotes HR (Batenburg et al.,

Journal of Cell Science (2020) 133, jcs234914. doi:10.1242/jcs.234914

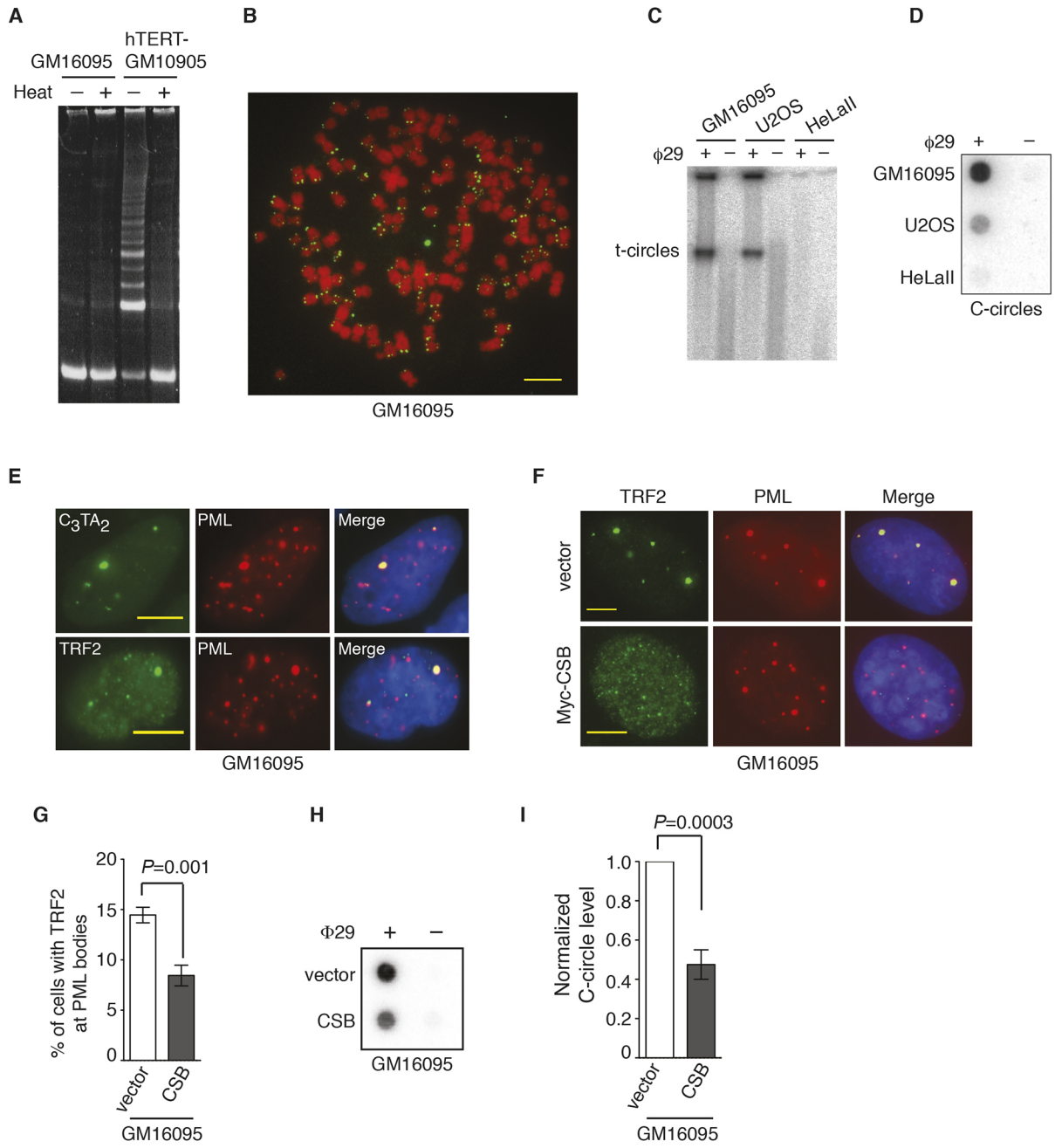

Fig. 1. Overexpression of CSB suppresses APBs and C-circles in SV40 transformed CSB-deficient patient GM16095 cells. (A) GM16095 cells do not exhibit any detectable telomerase activity. Ten thousand GM16095 or hTERT-GM10905 cells were used to measure telomerase activity. (B) A representative image of metaphase chromosome spreads from GM16095 cells. Chromosomes were stained with DAPI and false colored in red. Telomeric DNA was detected by FISH using a FITC-conjugated (CCCTAA)3-containing PNA probe (green). (C) T-circle analysis of GM16095 along with U2OS (positive control) and telomerase-expressing HeLaII cells (negative control). (D) C-circle analysis of GM16095 along with U2OS (positive control) and telomerase-expressing HeLaII cells (negative control). (E) Representative images of GM16095 cells stained with an anti-PML antibody in conjunction with either a FITC-conjugated (CCCTAA)3-containing PNA probe (green) or an anti-TRF2 antibody. Cell nuclei were stained with DAPI in blue in this and subsequent figures. (F) Representative images of vector- and Myc-CSB-expressing GM16095 cells co-stained with anti-TRF2 and anti-PML antibodies. (G) Quantification of the percentage of vector- and Myc-CSB-expressing GM16095 cells exhibiting colocalization of TRF2 with PML bodies. At least 1000 cells per experimental condition were scored in blind. Standard deviations from three independent experiments are indicated in this and subsequent panels. (H) A representative image of C-circles from vector- and Myc-CSB-expressing GM16095 cells. (I) Quantification of the level of C-circles from H. The C-circle signals were quantified with ImageQuant. The level of C-circles is represented in arbitrary units. The signal for Myc-CSB-expressing GM16095 cells was normalized relative to that for vector-expressing GM16095 cells. Scale bars: 5 µm.

2015, 2017). Therefore, we asked if CSB might be associated with ALT telomeres to regulate telomeric recruitment of HR repair proteins. IF analysis revealed that on average about 5% of asynchronous U2OS cells exhibited colocalization of CSB with telomere binding protein TRF2 (Fig. 3A), suggesting that CSB is associated with ALT telomeres. Further IF and IF-FISH analysis revealed that while MRE11, NBS1, BRCA1, BLM, RPA32 and POLD3 localized at ALT telomeres in U2OS WT cells (Fig. 3B), in

Journal of Cell Science (2020) 133, jcs234914. doi:10.1242/jcs.234914

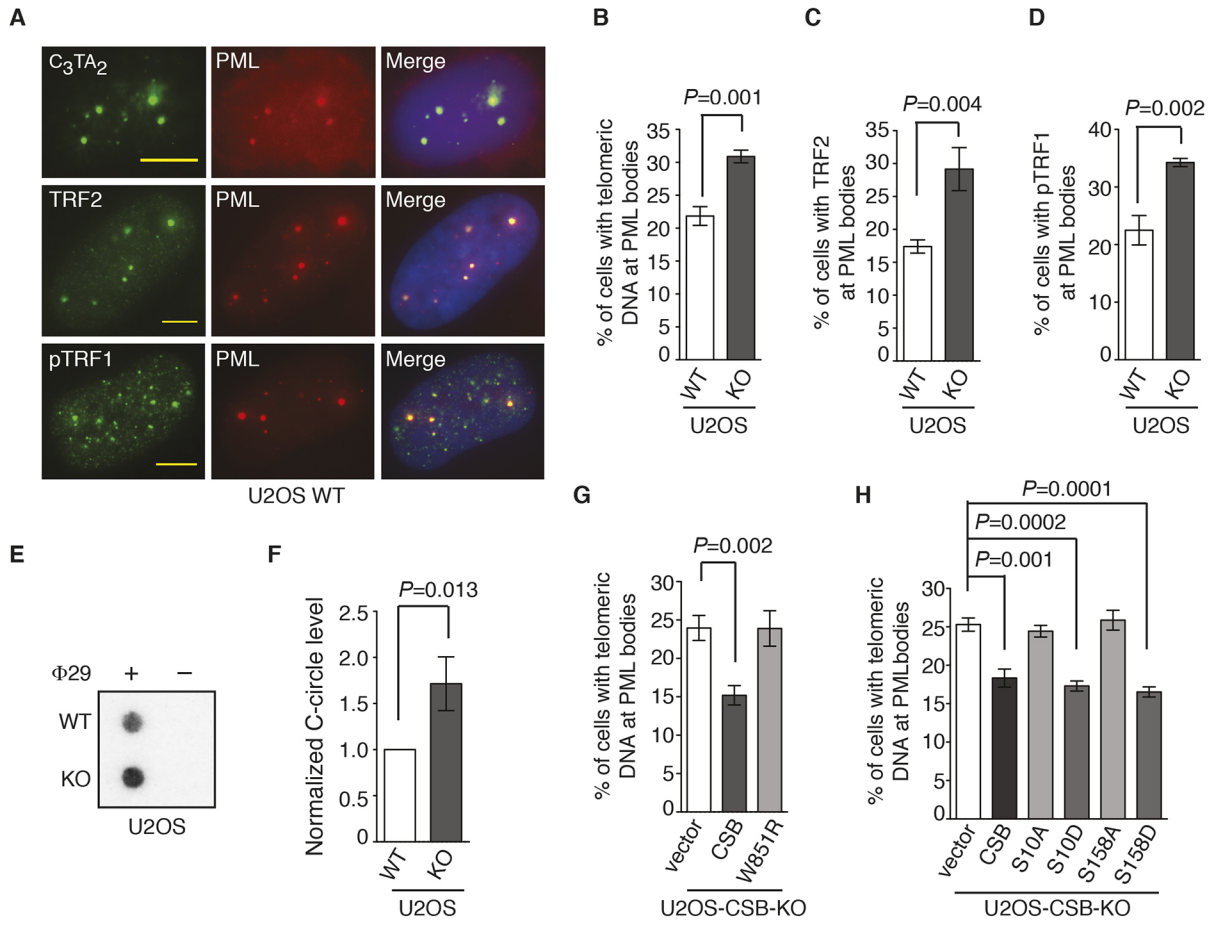

Fig. 2. CSB regulates APBs and C-circles in U2OS cells. (A) Representative images of U2OS cells stained with a mouse anti-PML antibody in conjunction with a FITC-conjugated-(CCCTAA)3 PNA probe (green), a rabbit anti-TRF2 or a rabbit anti-(pT371)TRF1 antibody. (B) Quantification of the percentage of cells exhibiting colocalization of telomeric DNA with PML bodies. U2OS WT and CSB-KO cells were costained with a FITC-conjugated-(CCCTAA)3 PNA probe and an anti-PML antibody. At least 1000 cells per experimental condition were scored in blind. Standard deviations from three independent experiments are indicated in this and subsequent panels. (C) Quantification of the percentage of U2OS WT and CSB-KO cells exhibiting colocalization of TRF2 with PML bodies. Scoring was done as in B. (D) Quantification of the percentage of U2OS WT and CSB-KO cells exhibiting colocalization of (pT371)TRF1 with PML bodies. Scoring was done as in B. (E) A representative image of C-circles from U2OS WT and CSB-KO cells. (F) Quantification of the level of C-circles from E. The quantification was done with ImageQuant. The signal for U2OS CSB-KO was normalized relative to that for U2OS WT. (G) Quantification of the percentage of vector-, Myc-CSB- or Myc-CSB-W851R-expressing U2OS CSB-KO cells exhibiting colocalization of telomeric DNA with PML bodies. Staining and scoring was done as in B. (H) Quantification of the percentage of vector- or various Myc-CSB allele-expressing U2OS CSB-KO cells exhibiting colocalization of telomeric DNA with PML bodies. Staining and scoring was done as in B. Scale bars: 5 µm.

agreement with previous findings (Dilley et al., 2016; Grobelny et al., 2000; Wu et al., 2000; Zhang et al., 2019a), their telomeric localization was impaired in U2OS CSB-KO cells (Fig. 3C-H; Fig. S3A). Loss of CSB had little impact on the expression of these HR repair proteins (Fig. S3B). In addition, reintroduction of Myc-CSB wild type into U2OS CSB-KO cells rescued telomeric localization of these HR repair proteins (Fig. S4A-D). Furthermore, an increased localization of NBS1 and BRCA1 to ALT telomeres was also observed in Myc-CSB-expressing GM16095 cells compared to vector-expressing GM16095 cells (Fig. S4E,F). Overexpression of Myc-CSB did not affect the expression of NBS1 and BRCA1 in CSB-deficient GM16095 cells (Fig. S4G). These results altogether suggest that CSB promotes recruitment of HR repair proteins and POLD3 to ALT telomeres.

CSB requires its ATPase activity to promote recruitment of HR repair proteins to ALT telomeres

To investigate if the ATPase activity of CSB might be required to recruit HR repair proteins to ALT telomeres, we first examined telomeric localization of BRCA1 and NBS1 in U2OS CSB-KO cells stably expressing either the vector alone, Myc-CSB or Myc-CSB-W851R. IF-FISH analysis revealed that while overexpression of Myc-CSB rescued recruitment of BRCA1 and NBS1 to ALT telomeres in U2OS CSB-KO cells, overexpression of Myc-CSB-W851R failed to do so (Fig. 4A,B). The expression of Myc-CSB-W851R was comparable to that of Myc-CSB (Fig. S2D). These results suggest that the ATPase activity of CSB is necessary to promote recruitment of HR repair proteins to ALT telomeres. In support of this notion, we also observed that neither Myc-CSB-S10A nor Myc-CSB-S158A, both of which have been reported to be defective in promoting the ATPase-dependent chromatin remodeling activity of CSB (Batenburg et al., 2017), was able to rescue recruitment of BRCA1 and NBS1 to ALT telomeres in U2OS CSB-KO cells (Fig. 4C,D). On the other hand, Myc-CSB carrying a phosphomimic mutation of either S10D or S158D behaved like Myc-CSB wild type and rescued recruitment of BRCA1 and NBS1 to ALT telomeres (Fig. 4C,D). The inability of both Myc-CSB-S10A and Myc-CSB-S158A to promote recruitment of BRCA1 and

Journal of Cell Science (2020) 133, jcs234914. doi:10.1242/jcs.234914

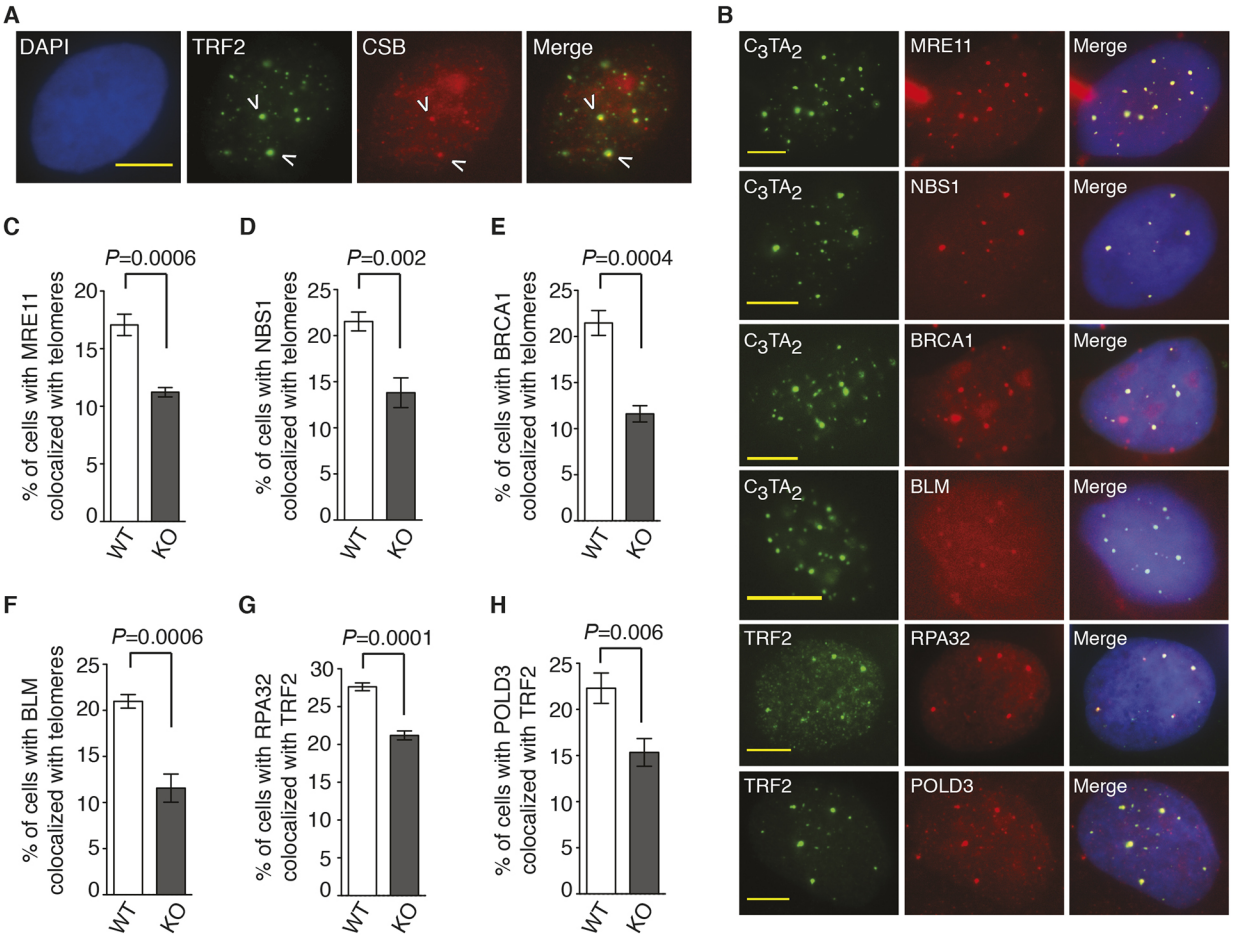

Fig. 3. CSB localizes to ALT telomeres and promotes telomeric recruitment of HR repair proteins and POLD3. (A) Representative images of U2OS cells immunostained with a mouse anti-CSB antibody in conjunction with a rabbit anti-TRF2 antibody. Arrowheads indicate colocalization of CSB with TRF2. (B) Representative images of IF and IF-FISH. For IF, U2OS WT cells were coimmunostained with an anti-TRF2 antibody in conjunction with either an anti-RPA32 or an anti-POLD3 antibody. For IF-FISH, U2OS WT cells were immunostained with a FITC-conjugated-(CCCTAA)3 PNA probe (green) in conjunction with an anti-MRE11, an anti-NBS1, an anti-BRCA1 or an anti-BLM antibody. (C) Quantification of the percentage of U2OS WT and CSB-KO cells exhibiting MRE11 colocalization with telomeres. At least 1000 cells per experimental condition were scored in blind in this and subsequent panels. Standard deviations from three independent experiments are indicated in this and subsequent panels. (D) Quantification of the percentage of U2OS WT and CSB-KO cells exhibiting NBS1 colocalization with telomeres. (E) Quantification of the percentage of U2OS WT and CSB-KO cells exhibiting BRCA1 colocalization with telomeres. (F) Quantification of the percentage of cells exhibiting BLM colocalization with telomeres. (G) Quantification of the percentage of U2OS WT and CSB-KO cells exhibiting RPA32 colocalization with TRF2. (H) Quantification of the percentage of U2OS WT and CSB-KO cells exhibiting colocalization of POLD3 with TRF2. Scale bars: 5 µm.

NBS1 to ALT telomeres was unlikely due to any defect in their expression (Fig. S2E). These results suggest that CSB phosphorylation on S10 by ATM and S158 by CDK2 controls its ability to promote recruitment of HR repair proteins to ALT telomeres.

CSB promotes telomere stability and prevents replication stress-induced telomere fragility

We observed that U2OS CSB-KO cells exhibited a significant increase in the telomeric accumulation of DNA damage marker γH2AX with TRF2 when compared to U2OS parental cells (Fig. 5A,B). This increase was suppressed when Myc-CSB wild type was reintroduced into U2OS CSB-KO cells (Fig. 5C), suggesting that CSB suppresses the formation of dysfunctional telomeres. To further investigate the role of CSB in regulating telomere stability, we performed FISH analysis of metaphase chromosomes from both U2OS WT and CSB-KO cells. We found that loss of CSB induced fragile telomeres and telomere loss (telomere signal-free ends) (Fig. 5D,E; Fig. S5). Reintroduction of Myc-CSB wild type into U2OS CSB-KO cells suppressed the formation of fragile telomeres and telomere loss (Fig. 5F,G). Taken together, these results suggest that CSB promotes telomere stability.

It has been well established that fragile telomeres arise from replication fork stalling (Martinez et al., 2009; Sfeir et al., 2009). Thus we asked if fragile telomeres and telomere loss induced in CSB-KO cells might be mediated by replication stress. To address this question, we treated both U2OS WT and CSB-KO cells with aphidicolin, which inhibits DNA polymerase. Treatment with aphidicolin led to a further induction in fragile telomeres in U2OS CSB-KO cells compared to U2OS WT cells (Fig. 5D), however it did not affect telomere loss (Fig. 5E). Reintroduction of Myc-CSB wild type into U2OS CSB-KO cells suppressed aphidicolin-induced formation of fragile telomeres (Fig. 5F) but not telomere loss (Fig. 5G). These results suggest that CSB prevents replication stress-induced formation of fragile telomeres.

CSB prevents accumulation of MUS81 and SLX4 at ALT telomeres

It has been reported that the structure-specific endonucleases MUS81-EME1 and SLX4-SLX1, which process stalled replication

Journal of Cell Science (2020) 133, jcs234914. doi:10.1242/jcs.234914

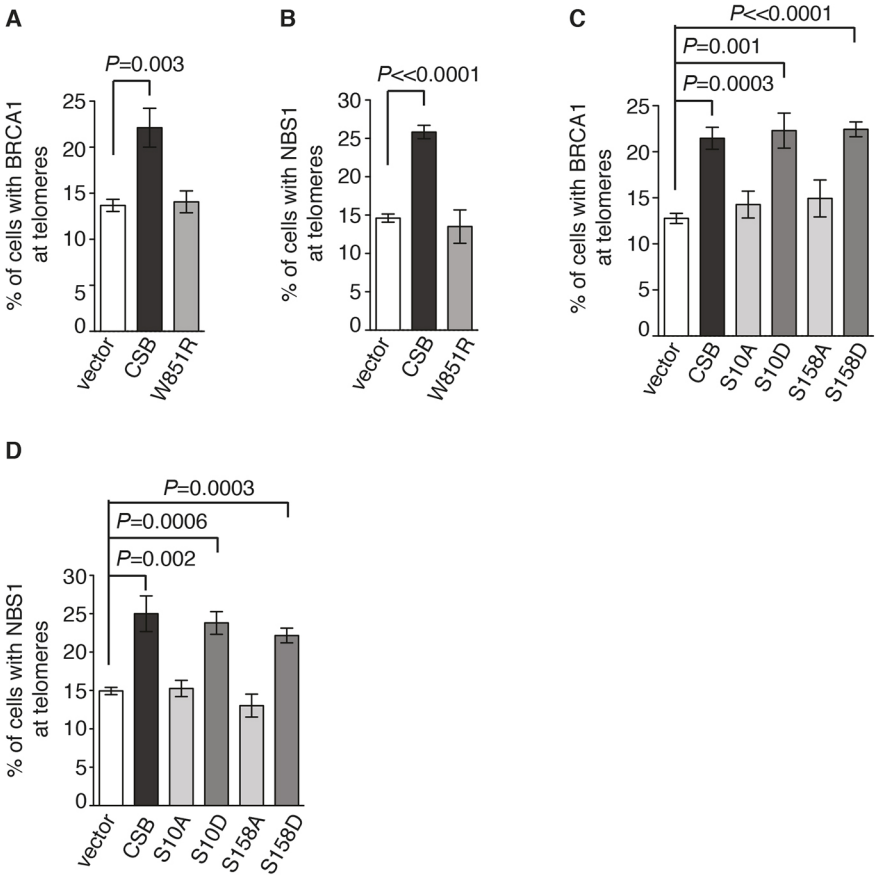

Fig. 4. CSB requires its ATPase activity to promote recruitment of HR repair proteins to ALT telomeres. (A) Quantification of the percentage of vector-, Myc-CSB- or Myc-CSB-W851R-expressing U2OS CSB-KO cells exhibiting BRCA1 localization at telomeres. Cells were costained with a FITC-conjugated-(CCCTAA)3 PNA probe and a rabbit anti-BRCA1 antibody. At least 1000 cells per experimental condition were scored in blind in this and subsequent panels. Standard deviations from three independent experiments are indicated in this and subsequent panels. (B) Quantification of the percentage of vector-, Myc-CSB- or Myc-CSB-W851R-expressing cells exhibiting NBS1 localization at telomeres. Cells were costained with a FITC-conjugated-(CCCTAA)3 PNA probe and a rabbit anti-NBS1 antibody. Scoring was done as in A. (C) Quantification of the percentage of vector- or various Myc-CSB allele-expressing U2OS CSB-KO cells exhibiting BRCA1 localization at telomeres. Staining and scoring were done as in A. (D) Quantification of the percentage of vector- or various Myc-CSB allele-expressing U2OS CSB-KO cells exhibiting NBS1 localization at telomeres. Staining and scoring were done as in B.

forks into DSBs (Fekairi et al., 2009; Hanada et al., 2007; Wyatt et al., 2013), are associated with ALT telomeres (Wan et al., 2013). Therefore, we asked if CSB might regulate recruitment of MUS81-EME1 and SLX4-SLX1 to ALT telomeres to process stalled replication intermediates arising from replication stress. IF and IF-FISH analysis revealed that MUS81 and SLX4 were readily found to localize to ALT telomeres in U2OS cells (Fig. 6A), in agreement with a previous finding (Wan et al., 2013). Loss of CSB increased their assocation with ALT telomeres in U2OS cells (Fig. 6B,C). Reintroduction of Myc-CSB wild type into U2OS CSB-KO cells suppressed telomeric association of MUS81 and SLX4 (Fig. 6D,E). In addition, reintroduction of Myc-CSB into CSB-deficient GM16095 cells also suppressed telomeric association of MUS81 (Fig. 6F). Taken together, these results suggest that CSB limits MUS-SLX-mediated processing of stalled forks at ALT telomeres.

Depletion of SMARCAL1 promotes telomeric recruitment of CSB

SMARCAL1, a chromatin remodeler, has been implicated in stabilizing stalled replication forks by catalyzing branch migration and fork regression (Bansbach et al., 2009; Betous et al., 2012; Yuan et al., 2009). It has been reported that depletion of SMARCAL1 leads to persistently stalled replication forks at ALT telomeres (Cox et al., 2016), which are processed by MUS81-EME1 and SLX1-SLX4. We reasoned that SMARCAL1-depleted cells represented a well-defined model to investigate the relationship of CSB with stalled forks at ALT telomeres. We transfected U2OS CSB-KO cells stably expressing Myc-CSB with either siControl or siSMARCAL1. IF analysis revealed that depletion of SMARCAL1 promoted telomeric association of Myc-CSB (Fig. 7A,B) but did not affect the expression of Myc-CSB in U2OS CSB-KO cells (Fig. S6A), suggesting that stalled replication forks trigger recruitment of CSB to ALT telomeres.

CSB and SMARCAL1 epistatically regulate APB formation

SMARCAL1 has been implicated in regulating the formation of APBs albeit with conflicting reports (Cox et al., 2016; Poole et al., 2015). Therefore, we asked if CSB and SMARCAL1 might act together to regulate APBs. To address this question, we depleted SMARCAL1 in both U2OS WT and CSB-KO cells (Fig. S6B). We observed that depletion of SMARCAL1 promoted APB formation in U2OS WT cells (Fig. 7C), in agreement with the previous finding from Flynn's group (Cox et al., 2016). Depletion of SMARCAL1 did not further induce APB formation in U2OS CSB-KO cells (Fig. 7C), suggesting that CSB and SMARCAL1 epistatically regulate APB formation.

CSB and SMARCAL1 cooperate to limit telomeric accumulation of γH2AX and MUS81

We observed that while depletion of SMARCAL1 induced telomeric accumulation of DNA damage marker γH2AX and MUS81 in U2OS WT cells (Fig. 7D,E), in agreement with a previous report that SMARCAL1 inhibits processing of stalled forks into DNA DSBs at ALT telomeres (Cox et al., 2016). Loss of CSB led to a further increase in telomeric accumulation of γH2AX and MUS81 in response to depletion of SMARCAL1 (Fig. 7D,E), suggesting that CSB and SMARCAL1 cooperatively prevent MUS81-mediated processing of stalled forks at ALT telomeres.

CSB does not mediate telomeric recruitment of HR repair proteins and POLD3 induced by depletion of SMARCAL1

It has been reported that DSBs arising from collapsed forks are channelled into homology-directed BIR repair (Costantino et al.,

Journal of Cell Science (2020) 133, jcs234914. doi:10.1242/jcs.234914

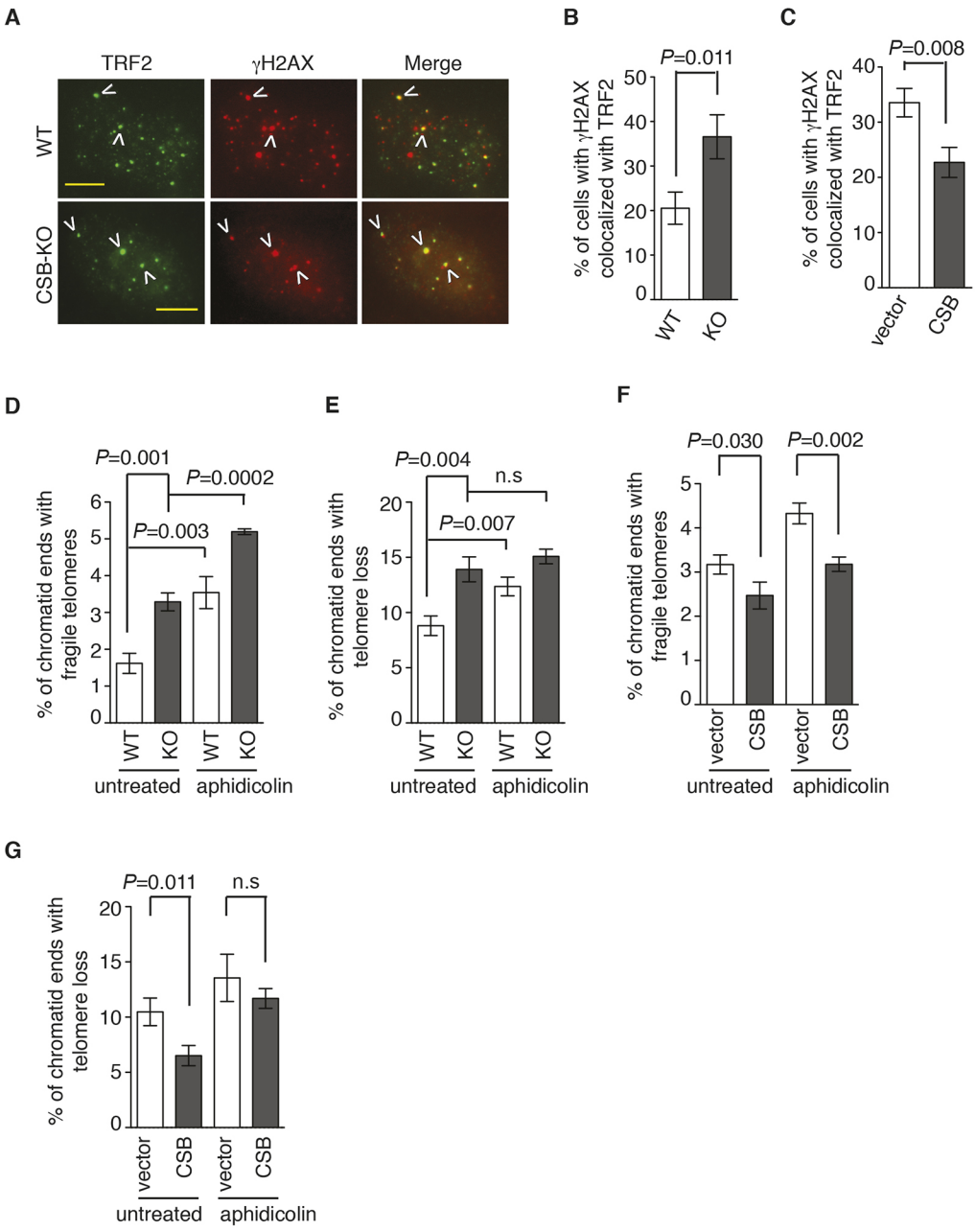

Fig. 5. CSB suppresses telomere fragility. (A) Representative images of U2OS WT and CSB-KO cells co-stained with anti-TRF2 and anti-γH2AX antibodies. Arrowheads indicate colocalization of TRF2 with γH2AX. (B) Quantification of U2OS WT and CSB-KO cells exhibiting colocalization of TRF2 and γH2AX. At least 250 cells per experimental condition was scored. Standard deviations from three independent experiments are indicated in this and subsequent panels. (C) Quantification of vector- or Myc-CSB-expressing U2OS CSB-KO cells exhibiting colocalization of TRF2 and γH2AX. A total of 160 cells per experimental condition was scored. (D,E) Quantification of fragile telomeres and telomere loss from U2OS WT and CSB-KO cells that were either untreated or treated with aphidicolin. For each cell line, a total of 42-53 metaphase cells were scored for the presence of fragile telomeres (D) and telomere loss (E). n.s: not significant. (F,G) Quantification of fragile telomeres and telomere loss from vector- or Myc-CSB-expressing U2OS CSB-KO cells that were either untreated or treated with aphidicolin. For each cell line, a total of 45-46 metaphase cells were scored for the presence of fragile telomeres (F) and telomere loss (G). n.s: not significant. Scale bars: 5 μm.

2014; Roumelioti et al., 2016). In agreement with these reports, we observed that depletion of SMARCAL1 led to an increase in telomeric accumulation of BRCA1, BLM, NBS1 and POLD3 in U2OS WT (Fig. 7F-I), suggesting that HR repair proteins and POLD3 are recruited to telomeres to repair DSBs arising from persistent replication stress in the absence of SMARCAL1 in ALT cells. We have shown that CSB promotes telomeric recruitment of HR repair proteins and POLD3 in ALT cells (Fig. 3). Therefore, we asked if CSB might mediate siSMARCAL1-induced recruitment of HR repair proteins and POLD3 to ALT telomeres. To address this question, we depleted SMARCAL1 in U2OS CSB-KO cells in addition to U2OS WT. Loss of CSB did not affect siSMARCAL1-induced recruitment of BRCA1, BLM, NBS1 and POLD3 to telomeres in U2OS cells (Fig. 7F-I). These results suggest that CSB does not mediate siSMARCAL1-induced recruitment of HR repair proteins and POLD3 to ALT telomeres.

CSB and SMARCAL1 make concerted efforts to prevent fragile telomeres and chromatid breaks

To further investigate cooperative roles of CSB and SMARCAL1 at ALT telomeres, we examined telomere abnormalities in both U2OS WT and CSB-KO cells depleted for SMARCAL1. FISH analysis of metaphase chromosomes revealed that depletion of SMARCAL1 promoted the formation of fragile telomeres in U2OS WT cells (Fig. 8A). Depletion of SMARCAL1 also led to a slight but insignificant increase in telomere loss in U2OS WT cells (Fig. 8B). Fragile telomeres but not telomere loss was further exacerbated in U2OS CSB-KO cells depleted for SMARCAL1 (Fig. 8A,B). These results suggest that CSB and SMARCAL1 cooperate with each other to prevent telomere fragility.

In addition to fragile telomeres, we also observed a synergistic induction of chromatid breaks in U2OS CSB-KO cells depleted for SMARCAL1 compared to either U2OS WT cells depleted for SMARCAL1 or U2OS CSB-KO cells alone (Fig. 8C). Depletion

Journal of Cell Science (2020) 133, jcs234914. doi:10.1242/jcs.234914

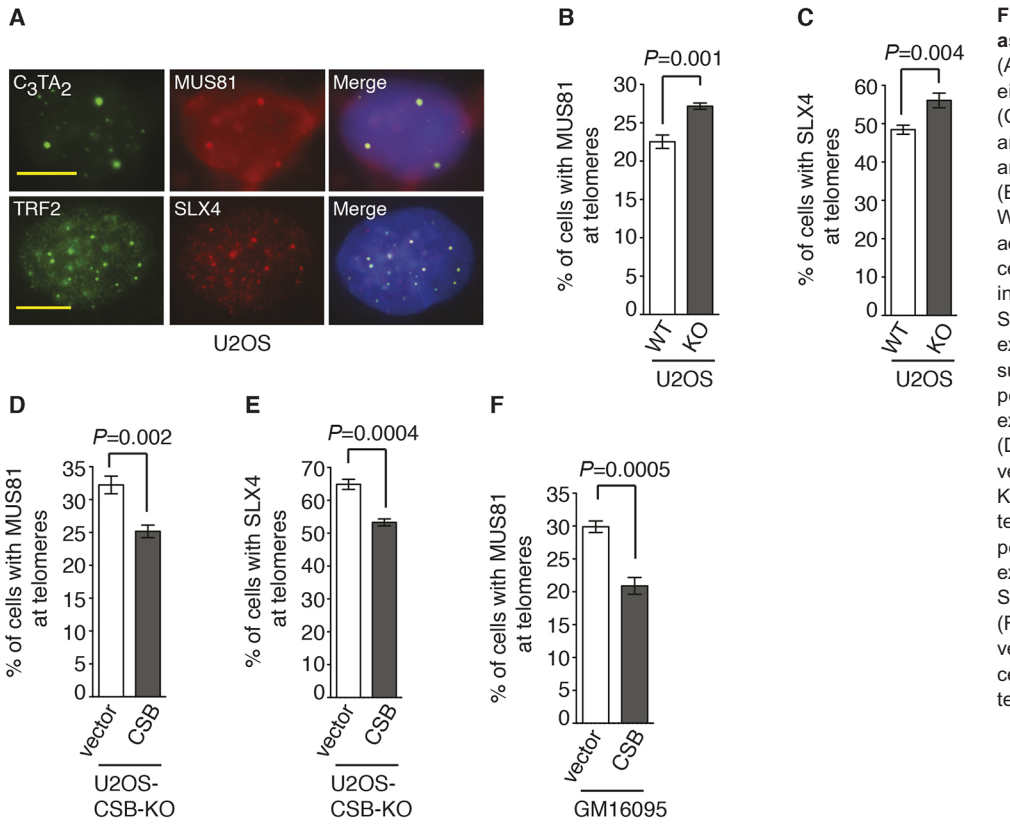

Fig. 6. CSB suppresses telomeric association of MUS81 and SLX4. (A) Representative images of U2OS cells either co-stained with a FITC-conjugated-(CCCTAA)3 PNA probe and an anti-MUS81 antibody or coimmunostained with anti-TRF2 and anti-SLX4 antibodies. (B) Quantification of the percentage of U2OS WT and CSB-KO cells exhibiting MUS81 accumulation at telomeres. At least 1000 cells per experimental condition were scored in blind in this and subsequent panels. Standard deviations from three independent experiments are indicated in this and subsequent panels. (C) Quantification of the percentage of U2OS WT and CSB-KO cells exhibiting SLX4 accumulation at telomeres. (D) Quantification of the percentage of vector- or Myc-CSB-expressing U2OS CSB-KO cells exhibiting MUS81 accumulation at telomeres. (E) Quantification of the percentage of vector- or Myc-CSB-expressing U2OS CSB-KO cells exhibiting SLX4 accumulation at telomeres. (F) Quantification of the percentage of vector- or Myc-CSB-expressing GM16095 cells exhibiting MUS81 accumulation at telomeres. Scale bars: 5 µm.

of SMARCAL1 combined with loss of CSB also resulted in a synthetic induction in micronuclei formation (Fig. 8D), which was associated with a synergistic reduction in cell proliferation (Fig. 8E). These results suggest that CSB and SMARCAL1 cooperate with each other to promote genomic integrity and cell growth.

DISCUSSION

The work presented here has revealed that CSB coordinates with SMARCAL1 to synergistically prevent telomere fragility in ALT cells. In addition, we have shown that loss of CSB coupled with depletion of SMARCAL1 leads to a synergistic increase in chromatid breaks and micronuclei formation, indicative of cooperative roles of CSB and SMARCAL1 in the maintenance of genomic integrity. Furthermore, our finding that depletion of SMARCAL1 combined with loss of CSB results in a synthetic reduction in cell proliferation underscores the importance of their synergistic cooperation in promoting cell growth.

It has been suggested that depletion of SMARCAL1 leads to persistently stalled replication forks at ALT telomeres, which are processed by structure-specific endonucleases MUS81-EME1 and SLX1-SLX4 to generate DSBs (Cox et al., 2016). Our finding that depletion of SMARCAL1 promotes recruitment of CSB to ALT telomeres indicates that stalled replication forks trigger recruitment of CSB to ALT telomeres. Several lines of evidence suggest that CSB promotes HR repair to prevent stalled forks from being processed into fragile telomeres (Fig. 8F). Firstly, loss of CSB impairs recruitment of HR repair proteins the MRN complex, BLM, BRCA1 and RPA32 to ALT telomeres, suggesting that CSB promotes HR repair at ALT telomeres. Secondly, loss of CSB promotes recruitment of MUS81 and SLX4 to ALT telomeres, indicating that CSB prevents MUS-SLX-mediated processing of stalled forks. Thirdly, loss of CSB promotes the formation of fragile telomeres, reported to arise from replication fork stalling (Martinez et al., 2009; Sfeir et al., 2009). We have shown that loss of CSB impairs telomeric recruitment of POLD3, an essential component of BIR, suggesting that CSB may promote homology-directed BIR repair at ALT telomeres. In addition, we have shown that treatment with a DNA polymerase inhibitor aphidicolin exacerbates the formation of fragile telomeres in the absence of CSB, suggesting that CSB also suppresses the formation of fragile telomeres induced by exogenous replication stress.

It has been reported that SMARCAL1 catalyzes regression of stalled replication forks to protect stalled forks from collapsing (Bansbach et al., 2009; Betous et al., 2012; Yuan et al., 2009). We have shown that depletion of SMARCAL1 stimulates telomeric accumulation of MUS81 and γH2AX. In addition, this stimulation is further exacerbated in the absence of CSB. Furthermore, depletion of SMARCAL1 coupled with loss of CSB leads to a synergistic increase in the formation of fragile telomeres. Taken together, these findings led us to propose a model in which SMARCAL1-mediated fork regression cooperates with CSB-mediated HR repair to prevent stalled forks from being processed into fragile telomeres (Fig. 8F). Our finding that depletion of SMARCAL1 promotes telomeric recruitment of HR proteins and POLD3 independently of CSB suggests that fragile telomeres can also arise from CSB-independent HR repair of stalled/collapsed forks (Fig. 8F).

It has been reported that replication stress at telomeres triggers the processes leading to hallmarks of ALT cells including APBs (Cox et al., 2016; Poole et al., 2015; Zhang et al., 2019b). We have shown that depletion of SMARCAL1 in CSB-KO cells does not exacerbate APB formation but promotes further replication stress as evidenced by a synthetic increase in telomeric association of γH2AX and MUS81. How a further increase in replication stress at ALT

Journal of Cell Science (2020) 133, jcs234914. doi:10.1242/jcs.234914

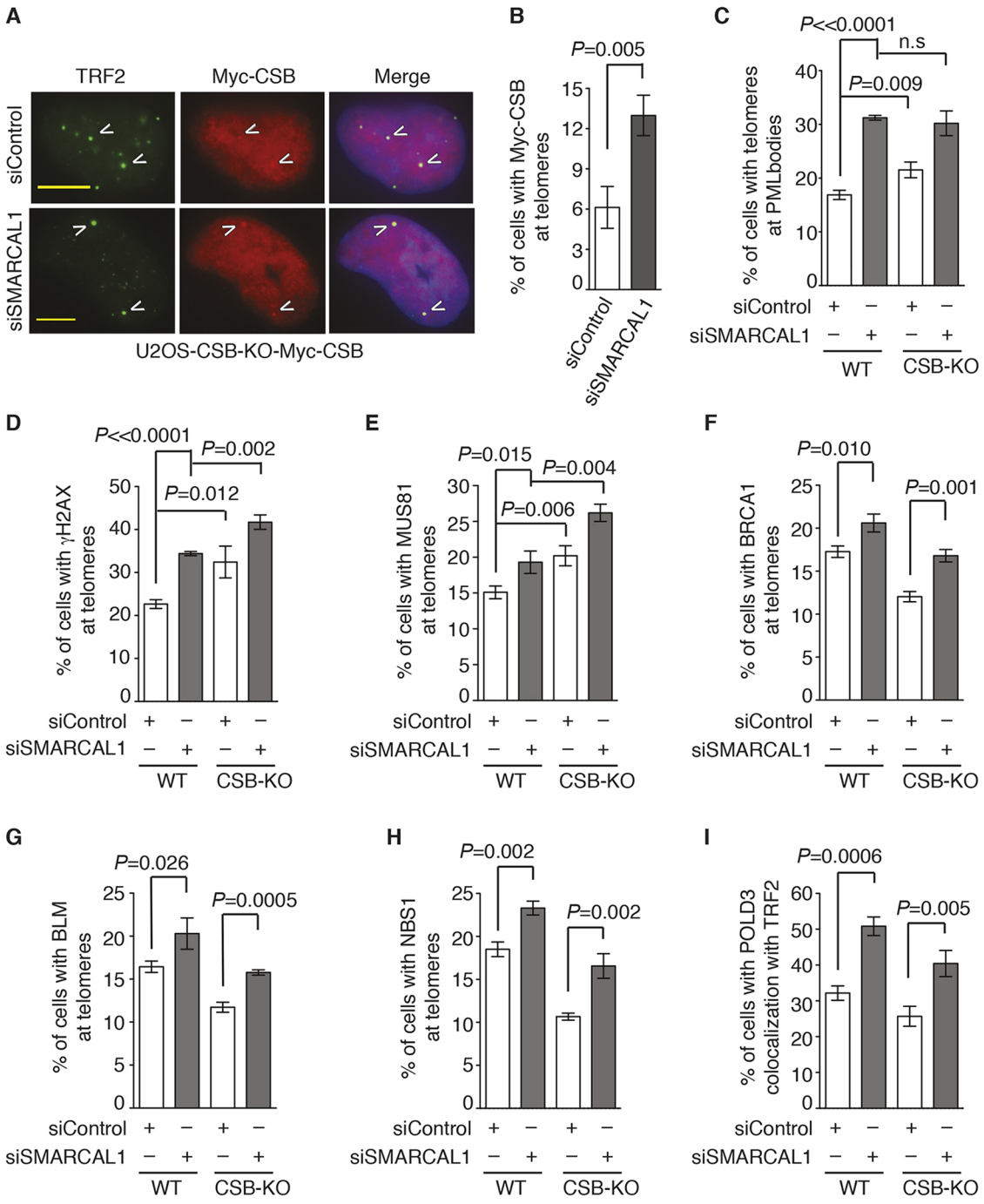

Fig. 7. Depletion of SMARCAL1 promotes telomeric recruitment of MUS81 and HR repair proteins, with the former exacerbated in the absence of CSB and the latter independent of CSB. (A) Representative images of Myc-CSB-expressing U2OS CSB-KO cells transfected with siControl or siSMARCAL1. Cells were coimmunostained with anti-TRF2 and anti-Myc antibodies. (B) Quantification of the percentage of cells exhibiting colocalization of Myc-CSB with TRF2 from A. At least 1000 cells per experimental condition were scored in blind. Standard deviations from three independent experiments are indicated in this and subsequent panels. (C) Quantification of the percentage of cells exhibiting association of telomeric DNA with PML bodies. U2OS WT and CSB-KO cells transfected with siControl or siSMARCAL1 were costained with a FITC-conjugated-(CCCTAA)3 PNA probe and an anti-PML antibody. Scoring was done as in B. (D) Quantification of cells exhibiting colocalization of TRF2 and γH2AX. U2OS WT and CSB-KO cells transfected with siControl or siSMARCAL1 were co-immunostained with anti-TRF2 and anti-γH2AX antibodies. A total of 305-421 cells per experimental condition was scored. (E) Quantification of the percentage of cells exhibiting MUS81 accumulation at telomeres. U2OS WT and CSB-KO cells transfected with siControl or siSMARCAL1 were co-stained with a FITC-conjugated-(CCCTAA)3 PNA probe and an anti-MUS81 antibody. Scoring was done as in B. (F) Quantification of the percentage of cells exhibiting BRCA1 localization at telomeres. U2OS WT and CSB-KO cells transfected with siControl or siSMARCAL1 were costained with a FITC-conjugated-(CCCTAA)3 PNA probe and an anti-BRCA1 antibody. Scoring was done as in B. (G) Quantification of the percentage of cells exhibiting BLM localization at telomeres. U2OS WT and CSB-KO cells transfected with siControl or siSMARCAL1 were costained with a FITC-conjugated-(CCCTAA)3 PNA probe and an anti-BLM antibody. Scoring was done as in B. (H) Quantification of the percentage of cells exhibiting NBS1 localization at telomeres. U2OS WT and CSB-KO cells transfected with siControl or siSMARCAL1 were costained with a FITC-conjugated-(CCCTAA)3 PNA probe and an anti-NBS1 antibody. Scoring was done as in B. (I) Quantification of the percentage of cells exhibiting POLD3 colocalization with TRF2. U2OS WT and CSB-KO cells transfected with siControl or siSMARCAL1 were costained with anti-TRF2 and anti-POLD3 antibodies. Scoring was done as in B. Scale bars: 5 µm.

Journal of Cell Science (2020) 133, jcs234914. doi:10.1242/jcs.234914

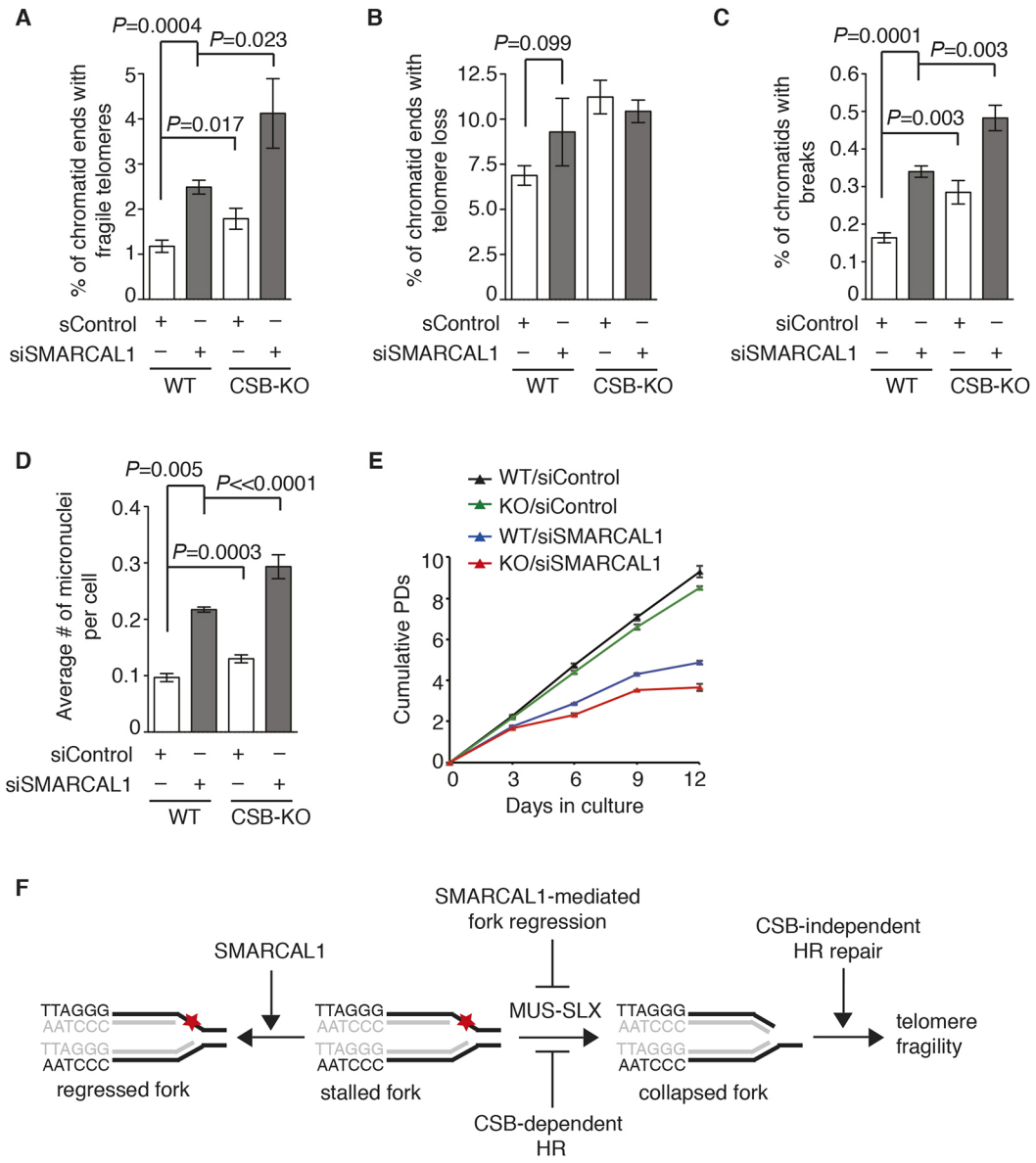

Fig. 8. CSB and SMARCAL1 cooperatively promote telomere stability, genomic integrity and cell proliferation. (A,B) Quantification of fragile telomeres and telomere loss from U2OS WT and CSB-KO cells transfected with siControl or siSMARCAL1. For each cell line, a total of 1794-2666 chromosomes from 46-65 metaphase cells were scored for the presence of fragile telomeres (A) and telomere loss (B). Standard deviations from three independent experiments are indicated in this and subsequent panels. (C) Quantification of chromatid breaks from U2OS WT and CSB-KO cells transfected with siControl or siSMARCAL1. For each cell line, a total of 2125-2382 chromosomes from 47-57 metaphase cells were scored for the presence of chromatid breaks. (D) Quantification of an average number of micronuclei per cell from U2OS WT and CSB-KO cells transfected with siControl or siSMARCAL1. A total of 1000 cells per experimental condition were scored in blind. (E) Cell proliferation assays of U2OS WT and CSB-KO cells transfected with siControl or siSMARCAL1. PD: population doubling. (F) Model for cooperative roles of CSB and SMARCAL1 in preventing telomere fragility. See the text for details.

telomeres fails to trigger a synthetic increase in APB formation in SMARCAL1-depleted CSB-KO cells is not known. Our finding that depletion of SMARCAL1 further exacerbates telomere fragility in CSB-KO cells suggests that replication stress arising from loss of CSB and SMARCAL1 impacts the formation of APBs in a manner mechanistically distinct from the formation of fragile telomeres.

It has been suggested that histone eviction by CSB serves as a prerequisite for active recruitment of BRCA1 by CSB to DSBs (Batenburg et al., 2019, 2017). Our finding that the ATPase-dead W851R mutation abrogates the ability of CSB to promote recruitment of BRCA1 and NBS1 to ALT telomeres suggests that CSB may remodel stalled/collapsed replication forks to facilitate recruitment of HR repair proteins to ALT telomeres. Previously we have reported that CSB is phosphorylated on S10 by ATM and on S158 by CDK2 and that these two phosphorylation events control its ATP-dependent chromatin remodeling activity at DSBs (Batenburg et al., 2017). We have shown that CSB carrying either a S10A or a S158A mutation fails to promote BRCA1 and NBS1 to ALT telomeres, suggesting that the chromatin remodeling activity of CSB at stalled/collapsed replication forks is likely mediated by ATM and CDK activities. It has been reported that ATR phosphorylates SMARCAL1 to prevent replication fork collapse (Couch et al., 2013). Together, these findings suggest that ATM and ATR may regulate the concerted actions of CSB and SMARCAL1 at ALT telomeres to prevent telomere fragility.

MATERIALS AND METHODS

DNA constructs, siRNAs and antibodies

Retroviral expression constructs for wild-type CSB and CSB mutant alleles (W851R, S10A, S10D, S158A and S158D) have been previously described (Batenburg et al., 2015, 2017).

siRNA used were purchased from Dharmacon: non-targeting siRNA pool (D-001206-14-05); SMARCAL1 (D-013058-04-0002). siRNA transfection was performed with RNAiMAX (Invitrogen) according to the manufacturer's protocol.

Antibodies used include those against: TRF2 (1:250; Zhu et al., 2000) (a generous gift from Titia de Lange, Rockefeller University); (pT371)TRF1 (1:500; McKerlie and Zhu, 2011); MRE11 (1:5000) and NBS1 (1:10,000; Zhu et al., 2000) (kind gifts from John Petrini, Memorial Sloan-Kettering Cancer Center); PML (1:100; Santa Cruz, sc-966); PML (1:500; Abcam, ab53773); BRCA1 (1:10,000; Millipore, 07-434); RPA32 (1:200; Abcam, ab2175); γ-H2AX (1:2000; Millipore, 05-636); BLM (1:2000; Bethyl Laboratory, A300-110A), CSB (1:125; Fitzgerald, 10R-1587); CSB (1:1000; Bethyl Laboratory, A301-345A); Myc (1:1000; EMD Millipore, 9E10); SMARCAL1 (1:100; Santa Cruz, sc-166209), MUS81 (1;100; Santa Cruz, sc-47692); SLX4 (1:1000; Abnova, H00084464-B01P); POLD3 (1:500; Abnova, H00010714-M01) and γ-tubulin (1:20,000; GTU88, Sigma).

Cell culture and inhibitor treatment

Cells were grown in DMEM medium with 10% fetal bovine serum (FBS) for U2OS (ATCC), U2OS CSB-KO (Batenburg et al., 2017), GM16095 (Coriell Institute) (Batenburg et al., 2012), hTERT-GM10905 (Batenburg et al., 2012), HeLaII (McKerlie et al., 2012; Saltman et al., 1993) and phoenix cells, supplemented with non-essential amino acids, L-glutamine, 100 U/ml penicillin and 0.1 mg/ml streptomycin. Retroviral gene delivery was carried out as described (Batenburg et al., 2012; Mitchell et al., 2009) to generate stable cell lines. Aphidicolin (Sigma) was used at 0.5 µM.

IF and FISH

IF and IF-FISH were carried out essentially as described (Ho et al., 2016; Wilson et al., 2016). For IF except for POLD3 staining, cells seeded on coverslips were fixed directly in PBS-buffered 3% paraformaldehyde. For POLD3 staining, cells were preextracted with cold CSK buffer (10 mM PIPES [pH 7.0], 100 mM NaCl, 300 mM sucrose, 3 mM $MgCl_2$, 0.7% Triton X-100) for 10 min prior to fixation. Cell images were recorded on a Zeiss Axioplan 2 microscope with a Hammamatsu C4742-95 camera and processed using the Openlab software package. Cells were scored positive if they exhibited colocalization of one or more large telomeric foci (telomere clustering) with PML bodies or if they exhibited colocalization of at least 3 small telomere foci with PML bodies.

Metaphase chromosome spreads and FISH

Metaphase chromosome spreads were prepared as described (McKerlie et al., 2012; Mitchell et al., 2009). For drug treatment, U2OS WT and CSB-KO cells were treated with aphidicolin (0.5 µM) for 48 h prior to their arrest in nocodazole (0.1 µg/ml) for 4 h. For siRNA knockdown, U2OS WT and CSB-KO cells were transfected with siRNA against SMARCAL1 for 44 h, followed by their arrest in nocodazole (0.1 µg/ml) for 4 h.

FISH analysis on metaphase chromosome spreads was carried out as described (Batenburg et al., 2012). Slides with chromosome spreads were incubated with 0.5 µg/ml FITC-conjugated-$(CCCTAA)_3$ PNA probe (Biosynthesis) for 2 h at RT. Subsequently, slides were washed, counter-stained with 0.2 µg/ml DAPI, and embedded in 90% glycerol/10% PBS containing 1 mg/ml *p*-phenylenediamine (Sigma).

Telomere length analysis and C-circle amplication assays

Telomere length analysis was carried out as described (Mitchell et al., 2009). Plugs containing the digested 3 µg genomic DNA were loaded on a 1% agarose gel in 0.5X TBE. Gels were run for 20 h at 5.4 V/cm at a constant pulse time of 5 s using a CHEF DR-II pulsed-field apparatus (Bio-Rad). C-circle amplification assays were performed as described (Ho et al., 2016). Following heat inactivation of ϕ29 at 65°C for 20 min, samples were loaded on the dot blots. The detection of ϕ29-amplified telomeric DNA was done with a ^{32}P-end-labeled single-strand $(CCCTAA)_3$ probe. Blots were exposed to PhosphoImager screens and scanned using a Typhoon 9400 PhosphorImager (GE Healthcare).

Growth curve and other assays

For growth curve assays, U2OS WT and CSB-KO cells were seeded at 25,000 cells per well in a 24-well plate. The next day, cells were transfected with siControl or siSMARCAL1 with lipofectamine RNAiMAX according to the manufacturer's instruction. Forty-eight hours post transfection, cells were counted and reseeded at 25,000 cells per well. This cycle was repeated three more times until day 12.

Protein extracts and immunoblotting were performed as described (McKerlie et al., 2013; McKerlie and Zhu, 2011). The activity of telomerase in cells was determined as described (Mitchell et al., 2009) using a Trapeze telomerase detection kit (Chemicon) according to the manufacturer's protocol.

Statistical analysis

A two-tailed Student's *t*-test was used to derive all *P*-values.

Acknowledgements

We are grateful to Titia de Lange for the anti-TRF2 antibody and to John Petrini for anti-MRE11 and anti-NBS1 antibodies.

Competing interests

The authors declare no competing or financial interests.

Author contributions

Conceptualization: X.-D.Z., J.R.W.; Investigation: E.F., N.L.B., J.R.W., A.H., T.R.H.M., J.Q.; Writing - original draft: X.-D.Z.; Writing - review & editing: J.R.W., N.L.B.; Supervision: X.-D.Z.; Project administration: X.-D.Z.; Funding acquisition: X.-D.Z.

Funding

This work is supported by funding from the Canadian Institutes of Health Research and Natural Sciences and Engineering Research Council of Canada (NSERC) to X.-D.Z. (PJT159793 and RGPIN-05110-2016). E.F. was a holder of an Undergraduate Student Research Award from the NSERC.

Supplementary information

Supplementary information available online at
http://jcs.biologists.org/lookup/doi/10.1242/jcs.234914.supplemental

References

Azzalin, C. M., Reichenbach, P., Khoriauli, L., Giulotto, E. and Lingner, J. (2007). Telomeric repeat containing RNA and RNA surveillance factors at mammalian chromosome ends. *Science* **318**, 798-801. doi:10.1126/science.1147182

Bansbach, C. E., Betous, R., Lovejoy, C. A., Glick, G. G. and Cortez, D. (2009). The annealing helicase SMARCAL1 maintains genome integrity at stalled replication forks. *Genes Dev.* **23**, 2405-2414. doi:10.1101/gad.1839909

Batenburg, N. L., Mitchell, T. R., Leach, D. M., Rainbow, A. J. and Zhu, X.-D. (2012). Cockayne Syndrome group B protein interacts with TRF2 and regulates telomere length and stability. *Nucleic Acids Res.* **40**, 9661-9674. doi:10.1093/nar/gks745

Batenburg, N. L., Thompson, E. L., Hendrickson, E. A. and Zhu, X. D. (2015). Cockayne syndrome group B protein regulates DNA double-strand break repair and checkpoint activation. *EMBO J.* **34**, 1399-1416. doi:10.15252/embj.201490041

Batenburg, N. L., Walker, J. R., Noordermeer, S. M., Moatti, N., Durocher, D. and Zhu, X.-D. (2017). ATM and CDK2 control chromatin remodeler CSB to inhibit RIF1 in DSB repair pathway choice. *Nat. Commun.* **8**, 1921. doi:10.1038/s41467-017-02114-x

Batenburg, N. L., Walker, J. R., Coulombe, Y., Sherker, A., Masson, J. Y. and Zhu, X. D. (2019). CSB interacts with BRCA1 in late S/G2 to promote MRN- and CtIP-mediated DNA end resection. *Nucleic Acids Res.* **47**, 10678-10692. doi:10.1093/nar/gkz784

Betous, R., Mason, A. C., Rambo, R. P., Bansbach, C. E., Badu-Nkansah, A., Sirbu, B. M., Eichman, B. F. and Cortez, D. (2012). SMARCAL1 catalyzes fork regression and Holliday junction migration to maintain genome stability during DNA replication. *Genes Dev.* **26**, 151-162. doi:10.1101/gad.178459.111

Cesare, A. J. and Reddel, R. R. (2010). Alternative lengthening of telomeres: models, mechanisms and implications. *Nat. Rev. Genet.* **11**, 319-330. doi:10.1038/nrg2763

Costantino, L., Sotiriou, S. K., Rantala, J. K., Magin, S., Mladenov, E., Helleday, T., Haber, J. E., Iliakis, G., Kallioniemi, O. P. and Halazonetis, T. D. (2014).

Break-induced replication repair of damaged forks induces genomic duplications in human cells. *Science* **343**, 88-91. doi:10.1126/science.1243211

Couch, F. B., Bansbach, C. E., Driscoll, R., Luzwick, J. W., Glick, G. G., Betous, R., Carroll, C. M., Jung, S. Y., Qin, J., Cimprich, K. A. et al. (2013). ATR phosphorylates SMARCAL1 to prevent replication fork collapse. *Genes Dev.* **27**, 1610-1623. doi:10.1101/gad.214080.113

Cox, K. E., Maréchal, A. and Flynn, R. L. (2016). SMARCAL1 resolves replication stress at ALT telomeres. *Cell Reports* **14**, 1032-1040. doi:10.1016/j.celrep.2016.01.011

Dilley, R. L., Verma, P., Cho, N. W., Winters, H. D., Wondisford, A. R. and Greenberg, R. A. (2016). Break-induced telomere synthesis underlies alternative telomere maintenance. *Nature* **539**, 54-58. doi:10.1038/nature20099

Fekairi, S., Scaglione, S., Chahwan, C., Taylor, E. R., Tissier, A., Coulon, S., Dong, M.-Q., Ruse, C., Yates, J. R., III, Russell, P. et al. (2009). Human SLX4 is a Holliday junction resolvase subunit that binds multiple DNA repair/recombination endonucleases. *Cell* **138**, 78-89. doi:10.1016/j.cell.2009.06.029

Grobelny, J. V., Godwin, A. K. and Broccoli, D. (2000). ALT-associated PML bodies are present in viable cells and are enriched in cells in the G(2)/M phase of the cell cycle. *J. Cell Sci.* **113**, 4577-4585.

Hanada, K., Budzowska, M., Davies, S. L., van Drunen, E., Onizawa, H., Beverloo, H. B., Maas, A., Essers, J., Hickson, I. D. and Kanaar, R. (2007). The structure-specific endonuclease Mus81 contributes to replication restart by generating double-strand DNA breaks. *Nat. Sruct. Mol. Biol.* **14**, 1096-1104. doi:10.1038/nsmb1313

Henson, J. D. and Reddel, R. R. (2010). Assaying and investigating Alternative Lengthening of Telomeres activity in human cells and cancers. *FEBS Lett.* **584**, 3800-3811. doi:10.1016/j.febslet.2010.06.009

Ho, A., Wilson, F. R., Peragine, S. L., Jeyanthan, K., Mitchell, T. R. and Zhu, X.-D. (2016). TRF1 phosphorylation on T271 modulates telomerase-dependent telomere length maintenance as well as the formation of ALT-associated PML bodies. *Sci. Rep.* **6**, 36913. doi:10.1038/srep36913

Laugel, V., Dalloz, C., Durand, M., Sauvanaud, F., Kristensen, U., Vincent, M. C., Pasquier, L., Odent, S., Cormier-Daire, V., Gener, B. et al. (2009). Mutation update for the CSB/ERCC6 and CSA/ERCC8 genes involved in Cockayne syndrome. *Hum. Mutat.* **31**, 113-126. doi:10.1002/humu.21154

Martinez, P., Thanasoula, M., Munoz, P., Liao, C., Tejera, A., McNees, C., Flores, J. M., Fernandez-Capetillo, O., Tarsounas, M. and Blasco, M. A. (2009). Increased telomere fragility and fusions resulting from TRF1 deficiency lead to degenerative pathologies and increased cancer in mice. *Genes Dev.* **23**, 2060-2075. doi:10.1101/gad.543509

McKerlie, M. and Zhu, X.-D. (2011). Cyclin B-dependent kinase 1 regulates human TRF1 to modulate the resolution of sister telomeres. *Nat. Commun.* **2**, 371. doi:10.1038/ncomms1372

McKerlie, M., Lin, S. and Zhu, X.-D. (2012). ATM regulates proteasome-dependent subnuclear localization of TRF1, which is important for telomere maintenance. *Nucleic Acids Res.* **40**, 3975-3989. doi:10.1093/nar/gks035

McKerlie, M., Walker, J. R., Mitchell, T. R., Wilson, F. R. and Zhu, X.-D. (2013). Phosphorylated (pT371)TRF1 is recruited to sites of DNA damage to facilitate homologous recombination and checkpoint activation. *Nucleic Acids Res.* **41**, 10268-10282. doi:10.1093/nar/gkt775

Mitchell, T. R. H., Glenfield, K., Jeyanthan, K. and Zhu, X.-D. (2009). Arginine methylation regulates telomere length and stability. *Mol. Cell. Biol.* **29**, 4918-4934. doi:10.1128/MCB.00009-09

Poole, L. A., Zhao, R., Glick, G. G., Lovejoy, C. A., Eischen, C. M. and Cortez, D. (2015). SMARCAL1 maintains telomere integrity during DNA replication. *Proc. Natl. Acad. Sci. USA* **112**, 14864-14869. doi:10.1073/pnas.1510750112

Porro, A., Feuerhahn, S., Reichenbach, P. and Lingner, J. (2010). Molecular dissection of telomeric repeat-containing RNA biogenesis unveils the presence of distinct and multiple regulatory pathways. *Mol. Cell. Biol.* **30**, 4808-4817. doi:10.1128/MCB.00460-10

Roumelioti, F. M., Sotiriou, S. K., Katsini, V., Chiourea, M., Halazonetis, T. D. and Gagos, S. (2016). Alternative lengthening of human telomeres is a conservative DNA replication process with features of break-induced replication. *EMBO Rep.* **17**, 1731-1737. doi:10.15252/embr.201643169

Saltman, D., Morgan, R., Cleary, M. L. and de Lange, T. (1993). Telomeric structure in cells with chromosome end associations. *Chromosoma* **102**, 121-128. doi:10.1007/BF00356029

Sfeir, A., Kosiyatrakul, S. T., Hockemeyer, D., MacRae, S. L., Karlseder, J., Schildkraut, C. L. and de Lange, T. (2009). Mammalian telomeres resemble fragile sites and require TRF1 for efficient replication. *Cell* **138**, 90-103. doi:10.1016/j.cell.2009.06.021

Stavropoulos, D. J., Bradshaw, P. S., Li, X., Pasic, I., Truong, K., Ikura, M., Ungrin, M. and Meyn, M. S. (2002). The Bloom syndrome helicase BLM interacts with TRF2 in ALT cells and promotes telomeric DNA synthesis. *Hum. Mol. Genet.* **11**, 3135-3144. doi:10.1093/hmg/11.25.3135

Troelstra, C., van Gool, A., de Wit, J., Vermeulen, W., Bootsma, D. and Hoeijmakers, J. H. (1992). ERCC6, a member of a subfamily of putative helicases, is involved in Cockayne's syndrome and preferential repair of active genes. *Cell* **71**, 939-953. doi:10.1016/0092-8674(92)90390-X

Wan, B., Yin, J., Horvath, K., Sarkar, J., Chen, Y., Wu, J., Wan, K., Lu, J., Gu, P., Yu, E. Y. et al. (2013). SLX4 assembles a telomere maintenance toolkit by bridging multiple endonucleases with telomeres. *Cell Reports* **4**, 861-869. doi:10.1016/j.celrep.2013.08.017

Wilson, F. R., Ho, A., Walker, J. R. and Zhu, X.-D. (2016). Cdk-dependent phosphorylation regulates TRF1 recruitment to PML bodies and promotes C-circle production in ALT cells. *J. Cell Sci.* **129**, 2559-2572. doi:10.1242/jcs.186098

Wu, G., Lee, W.-H. and Chen, P.-L. (2000). NBS1 and TRF1 colocalize at PML bodies during late S/G2 phases in immortalized telomerase-negative cells: Implication of NBS1 in alternative lengthening of telomeres. *J. Biol. Chem.* **275**, 30618-30622. doi:10.1074/jbc.C000390200

Wu, G., Jiang, X., Lee, W. H. and Chen, P. L. (2003). Assembly of functional ALT-associated promyelocytic leukemia bodies requires Nijmegen Breakage Syndrome 1. *Cancer Res.* **63**, 2589-2595.

Wyatt, H. D. M., Sarbajna, S., Matos, J. and West, S. C. (2013). Coordinated actions of SLX1-SLX4 and MUS81-EME1 for Holliday junction resolution in human cells. *Mol. Cell* **52**, 234-247. doi:10.1016/j.molcel.2013.08.035

Yeager, T. R., Neumann, A. A., Englezou, A., Huschtscha, L. I., Noble, J. R. and Reddel, R. R. (1999). Telomerase-negative immortalized human cells contain a novel type of promyelocytic leukemia (PML) body. *Cancer Res.* **59**, 4175-4179.

Yuan, J., Ghosal, G. and Chen, J. (2009). The annealing helicase HARP protects stalled replication forks. *Genes Dev.* **23**, 2394-2399. doi:10.1101/gad.1836409

Zhang, J. M., Yadav, T., Ouyang, J., Lan, L. and Zou, L. (2019a). Alternative lengthening of telomeres through two distinct break-induced replication pathways. *Cell Reports* **26**, 955-968.e3. doi:10.1016/j.celrep.2018.12.102

Zhang, T., Zhang, Z., Shengzhao, G., Li, X., Liu, H. and Zhao, Y. (2019b). Strand break-induced replication fork collapse leads to C-circles, C-overhangs and telomeric recombination. *PLoS Genet.* **15**, e1007925. doi:10.1371/journal.pgen.1007925

Zhu, X.-D., Küster, B., Mann, M., Petrini, J. H. J. and Lange, T. (2000). Cell-cycle-regulated association of RAD50/MRE11/NBS1 with TRF2 and human telomeres. *Nat. Genet.* **25**, 347-352. doi:10.1038/77139

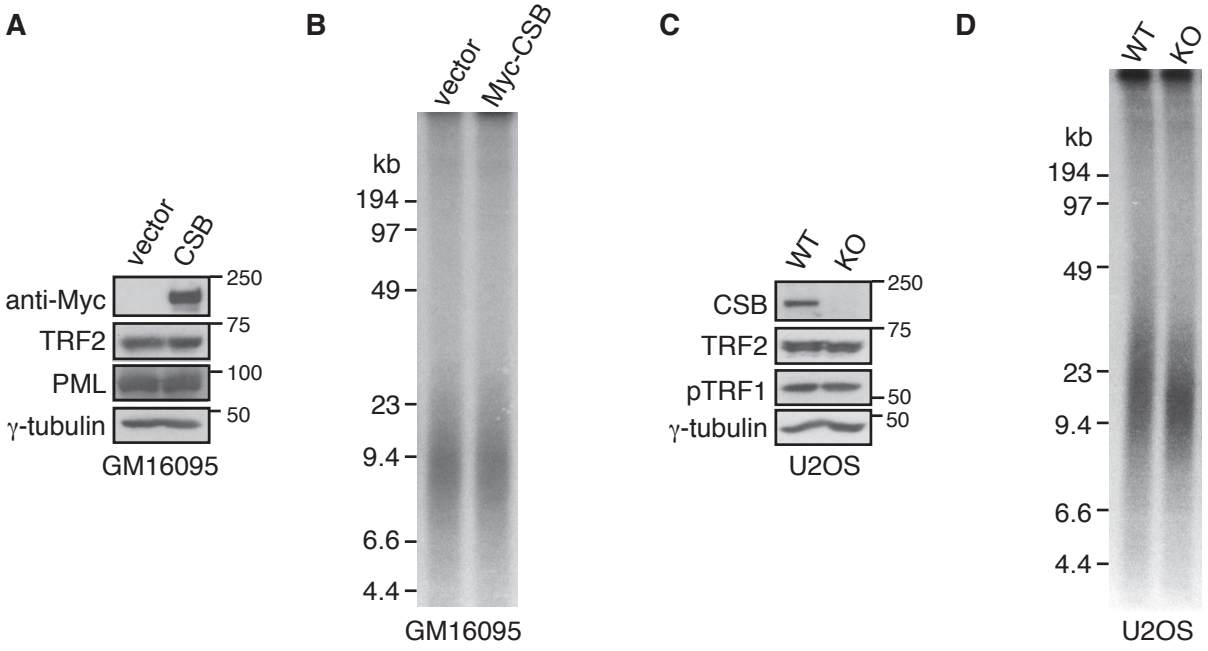

Figure S1. Loss of CSB does not affect telomere length heterogeneity in ALT cells. (**A**) Western analysis of vector- and Myc-CSB-expressing GM16095 cells. Immunoblotting was performed with anti-Myc, anti-TRF2, anti-PML and anti-γ-tubulin antibodies. The γ-tubulin blot was used as a loading control in this and subsequent figures. (**B**) Genomic blot of telomeric restriction fragments. RsaI/HinfI-digested genomic DNA (3 μg) from both vector- and Myc-CSB-expressing GM16095 cells was separated on a CHEF gel. The DNA molecular size markers are shown on the left of the blot. (**C**) Western analysis of U2OS WT and CSB-KO cells. Immunoblotting was performed with anti-CSB, anti-TRF2, anti-(pT371)TRF1 and anti-γ-tubulin antibodies. (**D**) Genomic blot of telomeric restriction fragments. RsaI/HinfI-digested genomic DNA (3 μg) from both U2OS WT and CSB-KO cells was separated on a CHEF gel. The DNA molecular size markers are shown on the left of the blot.

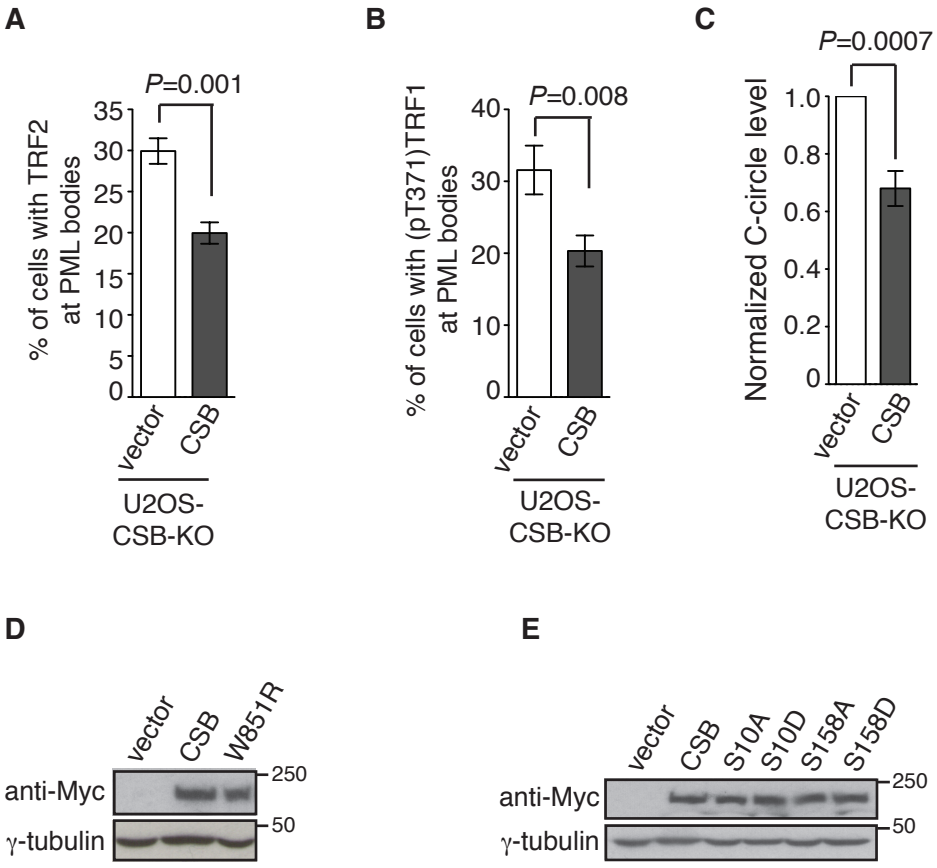

Figure S2. CSB regulates APB formation and C-circle production. (**A**) Quantification of the percentage of cells exhibiting colocalization of telomeric DNA with PML bodies. Vector- and Myc-CSB expressing U2OS CSB-KO cells were costained with a FITC-conjugated-(CCCTAA)3 PNA probe and an anti-PML antibody. At least 1000 cells per experimental condition were scored in blind. Standard deviations from three independent experiments are indicated in this and subsequent panels. (**B**) Quantification of the percentage of vector- and Myc-CSB expressing U2OS CSB-KO cells exhibiting colocalization of TRF2 with PML bodies. Scoring was done as in S2A. (**C**) Quantification of the percentage of vector- and Myc-CSB expressing U2OS CSB-KO cells exhibiting colocalization of (pT371)TRF1 with PML bodies. Scoring was done as in S2A. (**D**) Western analysis of U2OS CSB-KO cells expressing the vector alone, Myc-CSB WT or Myc-CSB-W851R. Immunoblotting was performed with anti-Myc and anti-γ-tubulin antibodies. (**E**) Western analysis of U2OS CSB-KO cells expressing the vector alone or various Myc-tagged CSB alleles as indicated. Immunoblotting was performed with anti-Myc and anti-γ-tubulin antibodies.

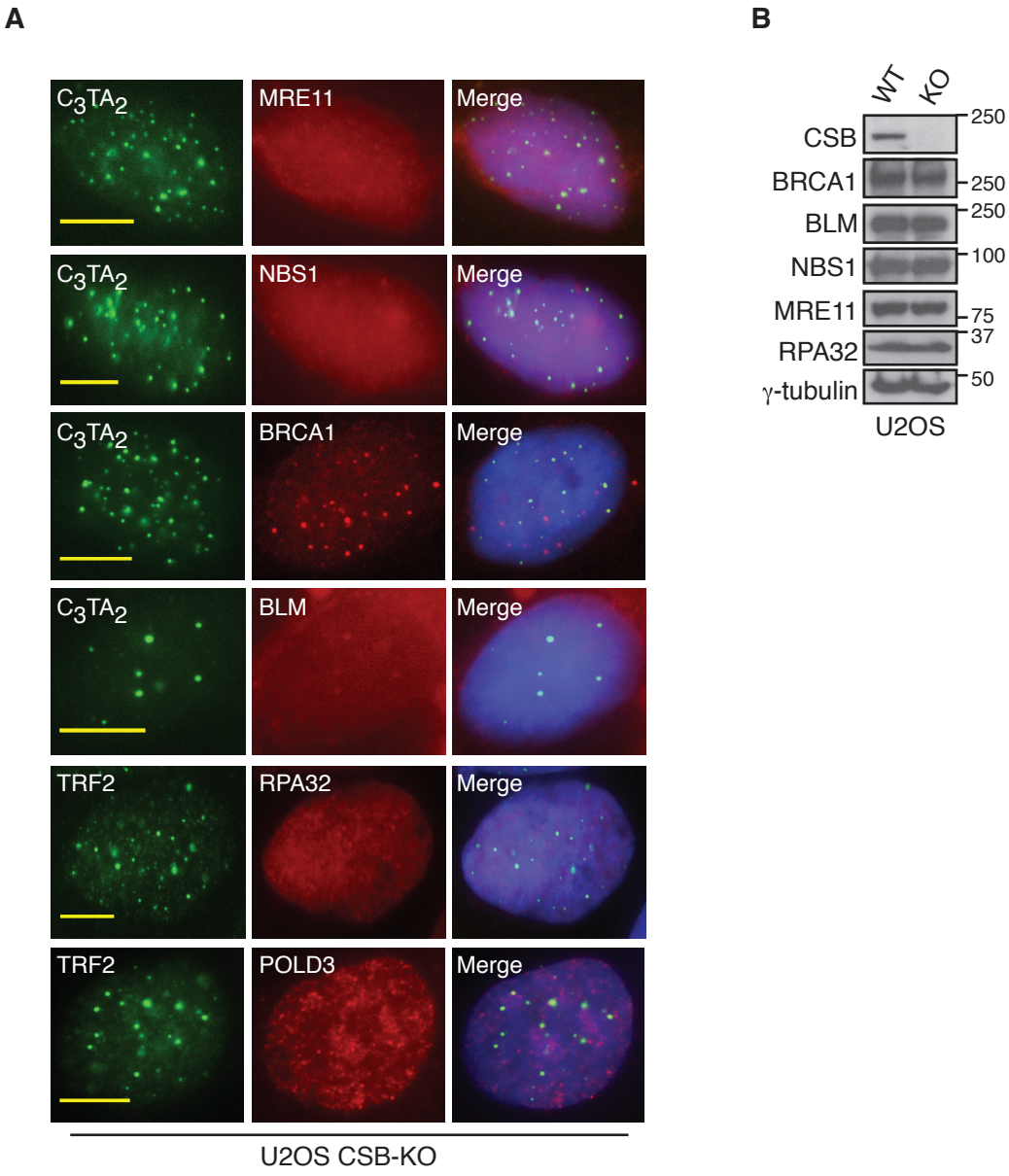

Figure S3. CSB promotes recruitment of HR repair proteins and POLD3 to ALT telomeres. (**A**) Representative images of IF and IF-FISH. For IF, U2OS CSB-KO cells were coimmunostained with an anti-TRF2 antibody in conjunction with either an anti-RPA32 or an anti-POLD3 antibody. For IF-FISH, U2OS CSB-KO cells were immunstained with a FITC-conjugated-(CCCTAA)3 PNA probe (green) in conjunction with an anti-MRE11, an anti-NBS1, an anti-BRCA1 or an anti-BLM antibody. (**B**) Western analysis of U2OS WT and CSB-KO cells. Immunoblotting was done with anti-CSB, anti-BRCA1, anti-BLM, anti-NBS1, anti-MRE11, anti-RPA32 and anti-γ-tubulin antibodies.

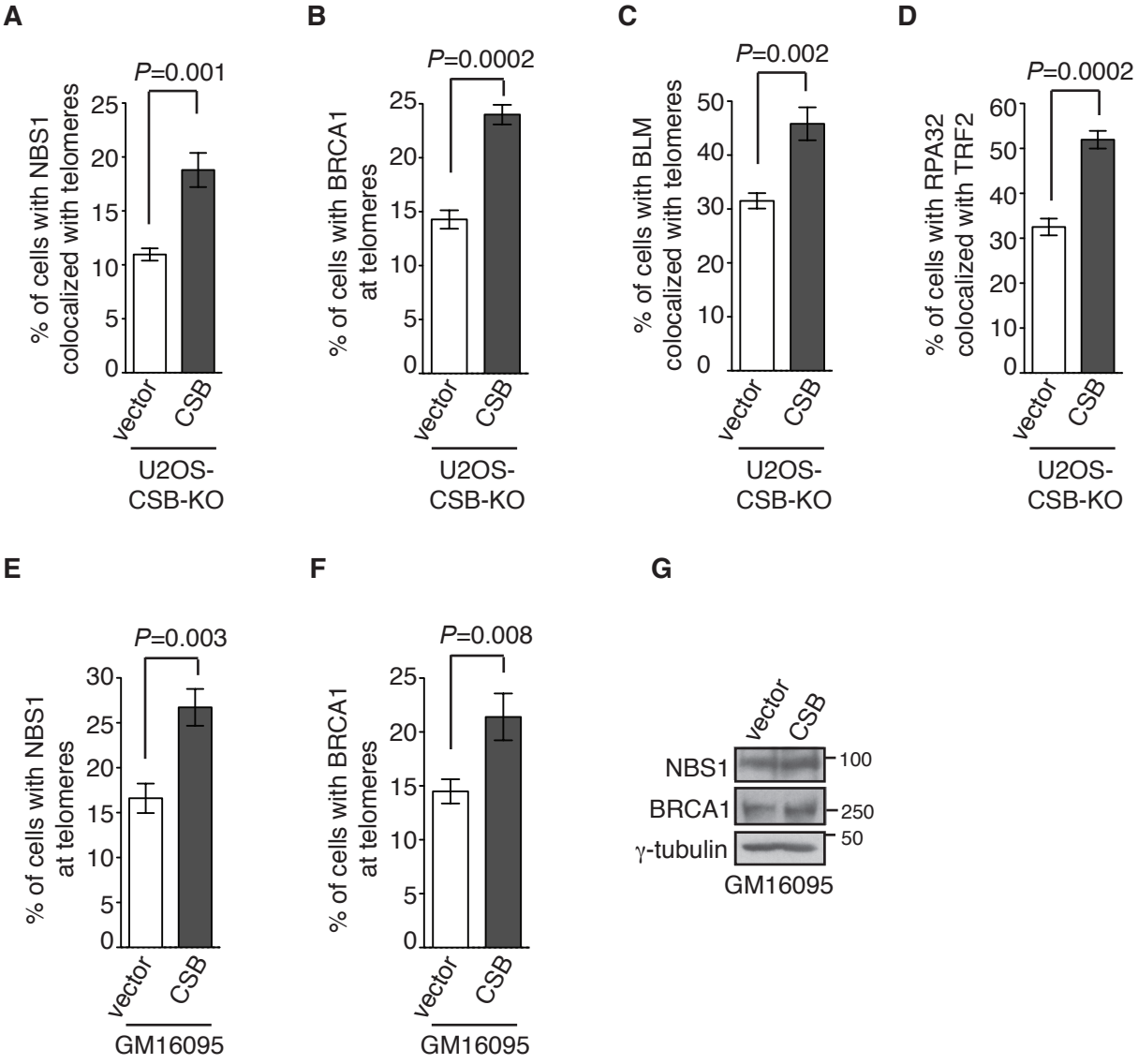

Figure S4. CSB promotes recruitment of HR repair proteins to ALT telomeres. (**A**) Quantification of the percentage of vector- and Myc-CSB-expressing U2OS CSB-KO cells exhibiting NBS1 colocalization with telomeres. At least 1000 cells per experimental condition were scored in blind in this and subsequent panels. Standard deviations from three independent experiments are indicated in this and subsequent panels. (**B**) Quantification of the percentage of vector- and Myc-CSB-expressing U2OS CSB-KO cells exhibiting BRCA1 colocalization with telomeres. (**C**) Quantification of the percentage of vector- and Myc-CSB-expressing U2OS CSB-KO cells exhibiting BLM colocalization with telomeres. (**D**) Quantification of the percentage of vector- and Myc-CSB-expressing U2OS CSB-KO cells exhibiting RPA32 colocalization with TRF2. (**E**) Quantification of the percentage of vector- and Myc-CSB-expressing GM16095 cells exhibiting NBS1 colocalization with telomeres. (**F**) Quantification of the percentage of vector- and Myc-CSB-expressing GM16095 cells exhibiting BRCA1 colocalization with telomeres. (**G**) Western analysis of vector- and Myc-CSB-expressing GM16095 cells. Immunoblotting was done with anti-NBS1, anti-BRCA1 and anti-γ-tubulin antibodies.

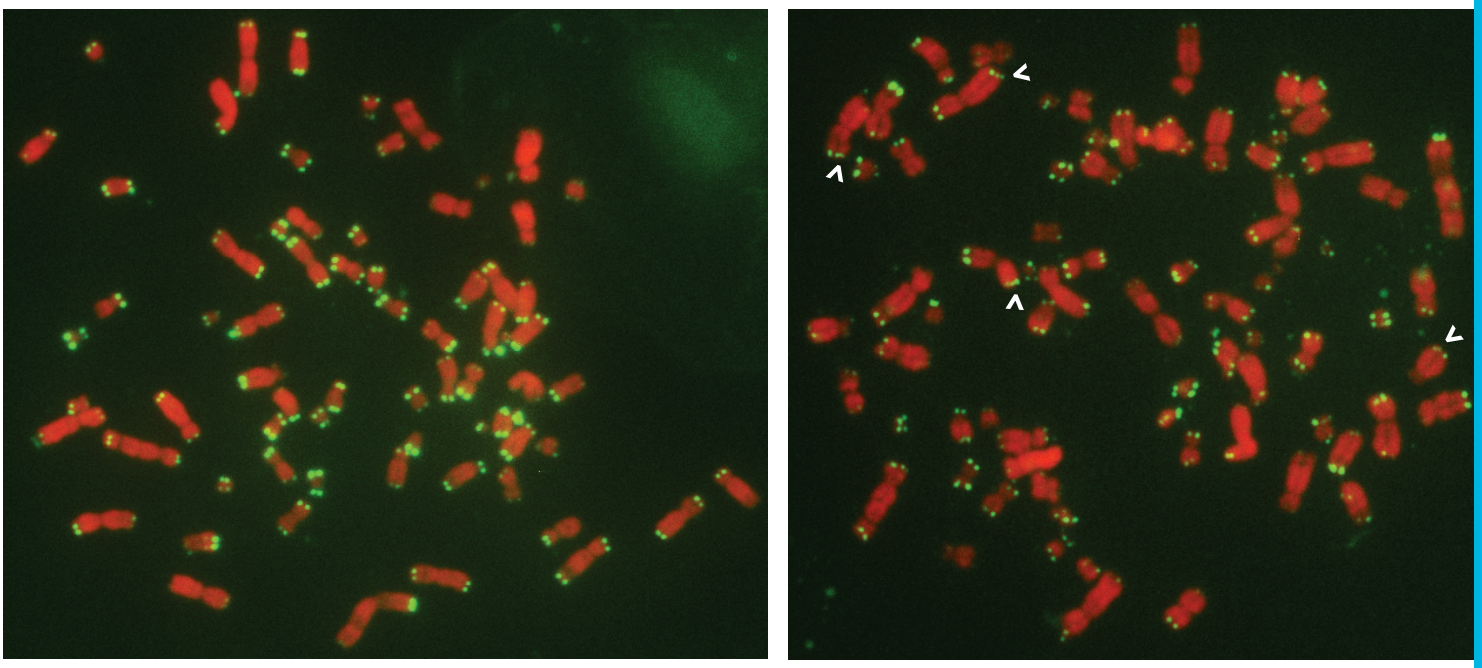

Figure S5. CSB suppresses telomere fragility. Representative images of metaphase chromosome spreads of U2OS WT and CSB-KO cells. Chromosomes were stained with DAPI and false colored in red. Telomeric DNA was detected by FISH using a FITC-conjugated (CCCTAA)3-containing PNA probe (green). Arrowheads indicate fragile telomeres.

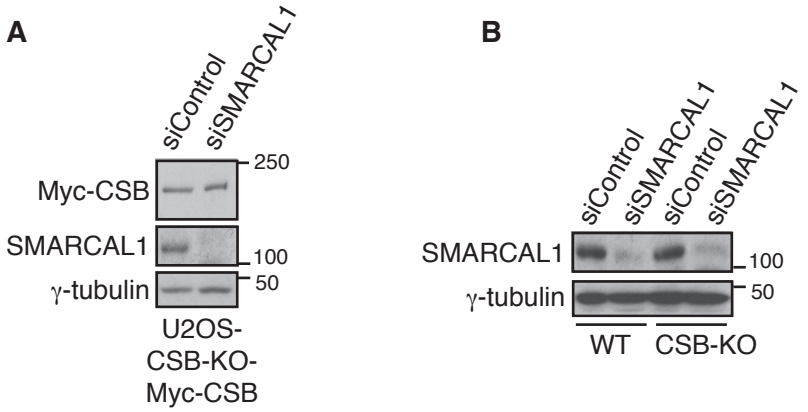

Figure S6. (**A**) Western analysis of Myc-CSB-expressing U2OS CSB-KO depleted for siControl or siSMARCAL1. Immunoblotting was done with anti-Myc, anti-SMARCAL1 and anti-γ-tubulin antibodies. (**B**) Western analysis of U2OS WT and CSB-KO cells transfected with siControl or siSMARCAL1. Immunoblotting was performed with anti-SMARCAL1 and anti-γ-tubulin antibodies.